Simulations, Clusters of Galaxies, and Cosmology: I. Introduction and Large-scale Structure Simulations

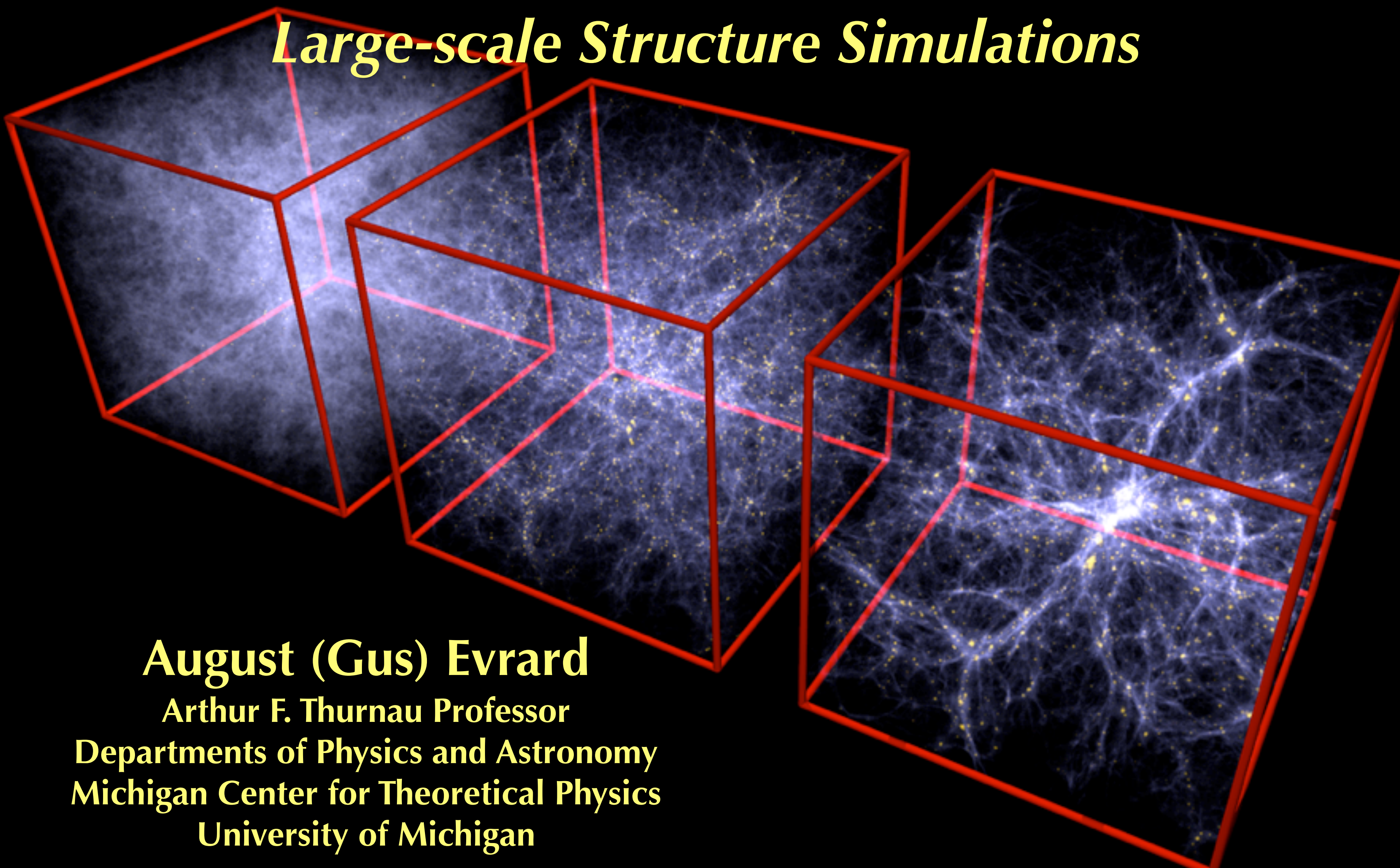

V. Springel & Virgo Consortium 2003

August (Gus) Evrard

Arthur F. Thurnau Professor

Departments of Physics and Astronomy

Michigan Center for Theoretical Physics

University of Michigan

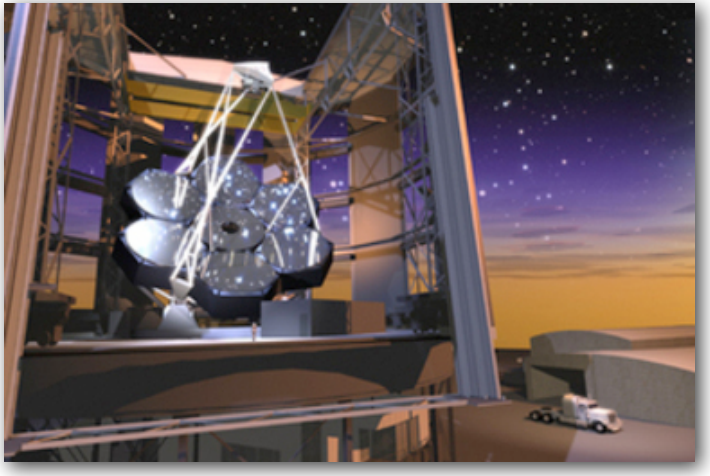

observation

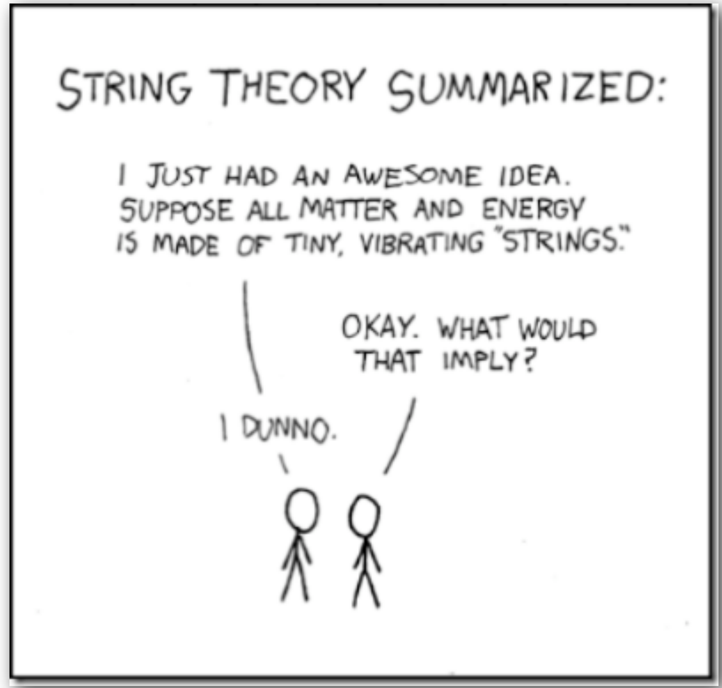

theory

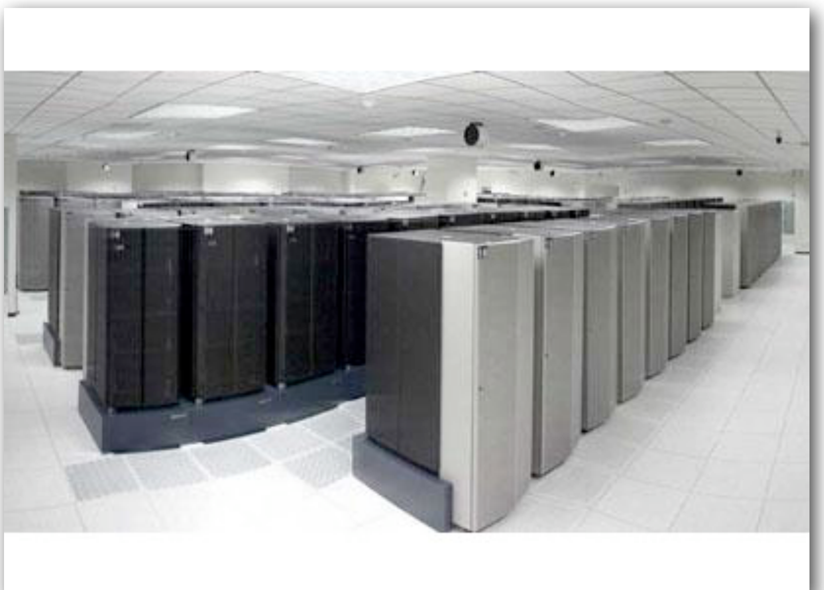

computation

The first three paradigms of scientific research

The fourth paradigm?

DATA-driven
scientific discovery

Phenomenology

outline:

* cosmic structure as a (complex!) initial-value problem
* Large-scale Structure (LSS) Simulations
  - methodologies, classes of problems
  - dark matter (DM) evolution: methods+results

Tomorrow:

  - DM + baryons: methods, results and challenges
  - galaxy formation: the never-ending story

* Cluster physics and phenomenology

* Cosmological studies with clusters of galaxies

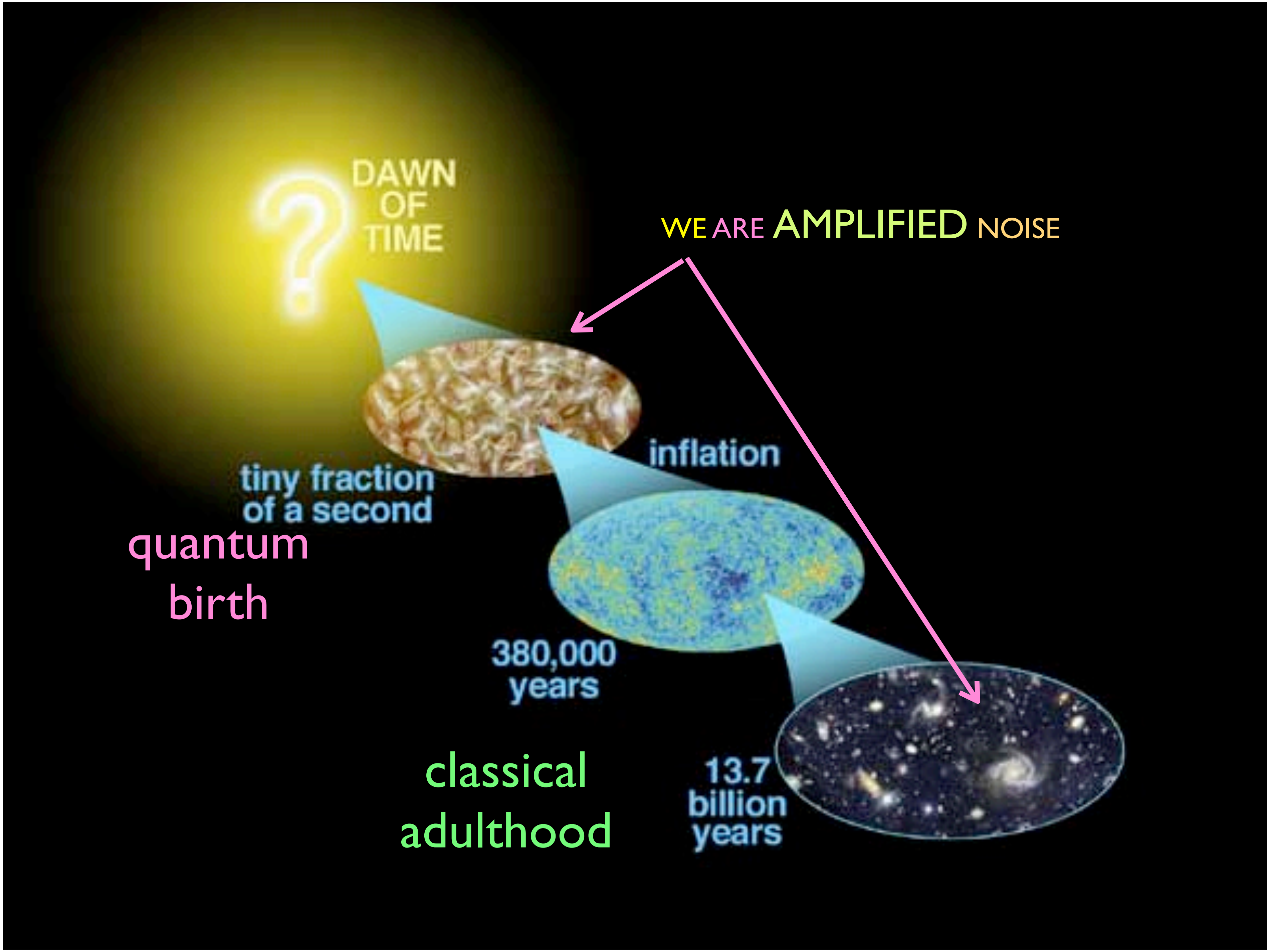
DAWN OF TIME
WE ARE AMPLIFIED NOISE
tiny fraction of a second
inflation
quantum birth
380,000 years
classical adulthood
13.7 billion years

Wilkinson Microwave
Anisotropy Probe
http://map.gsfc.nasa.gov

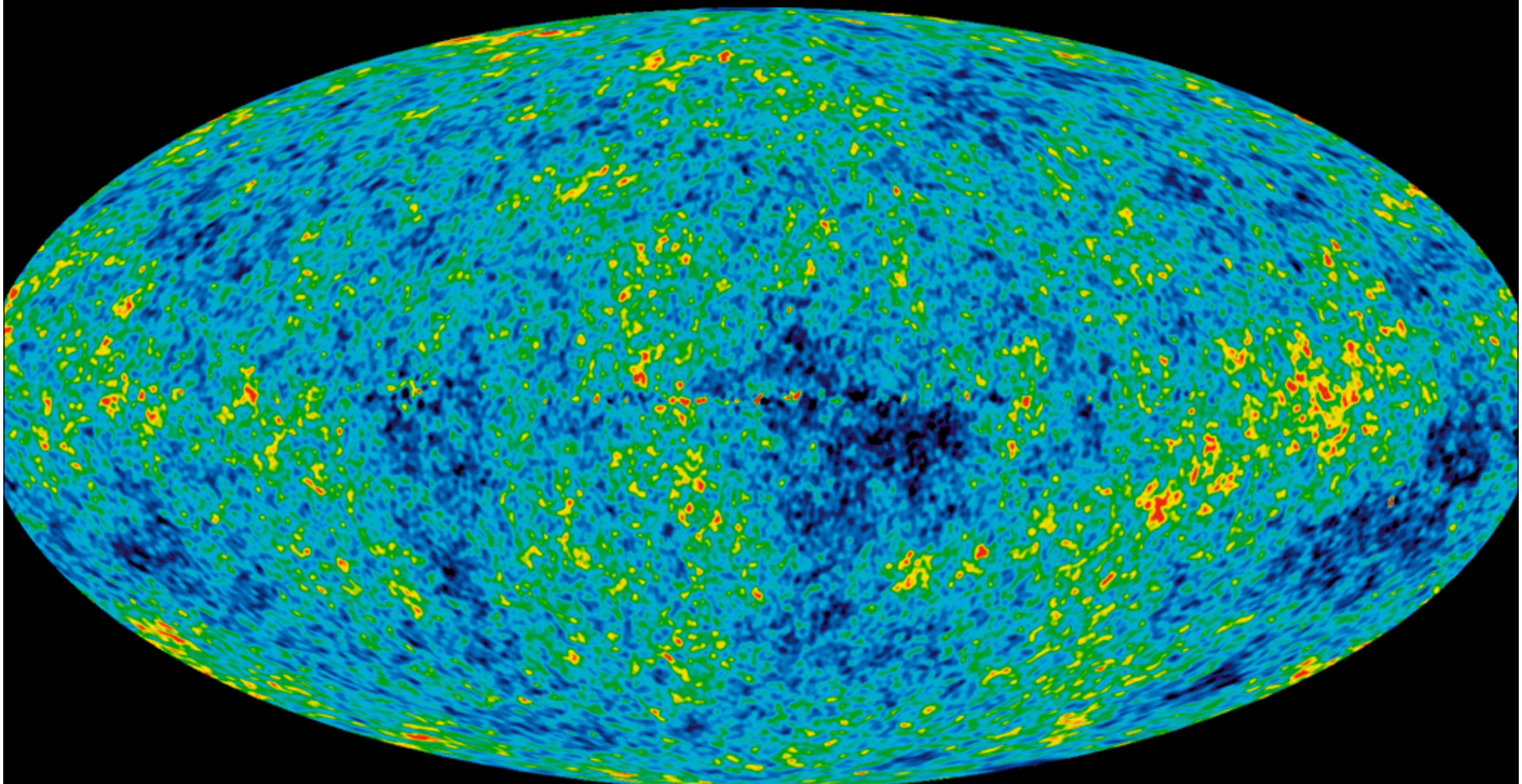

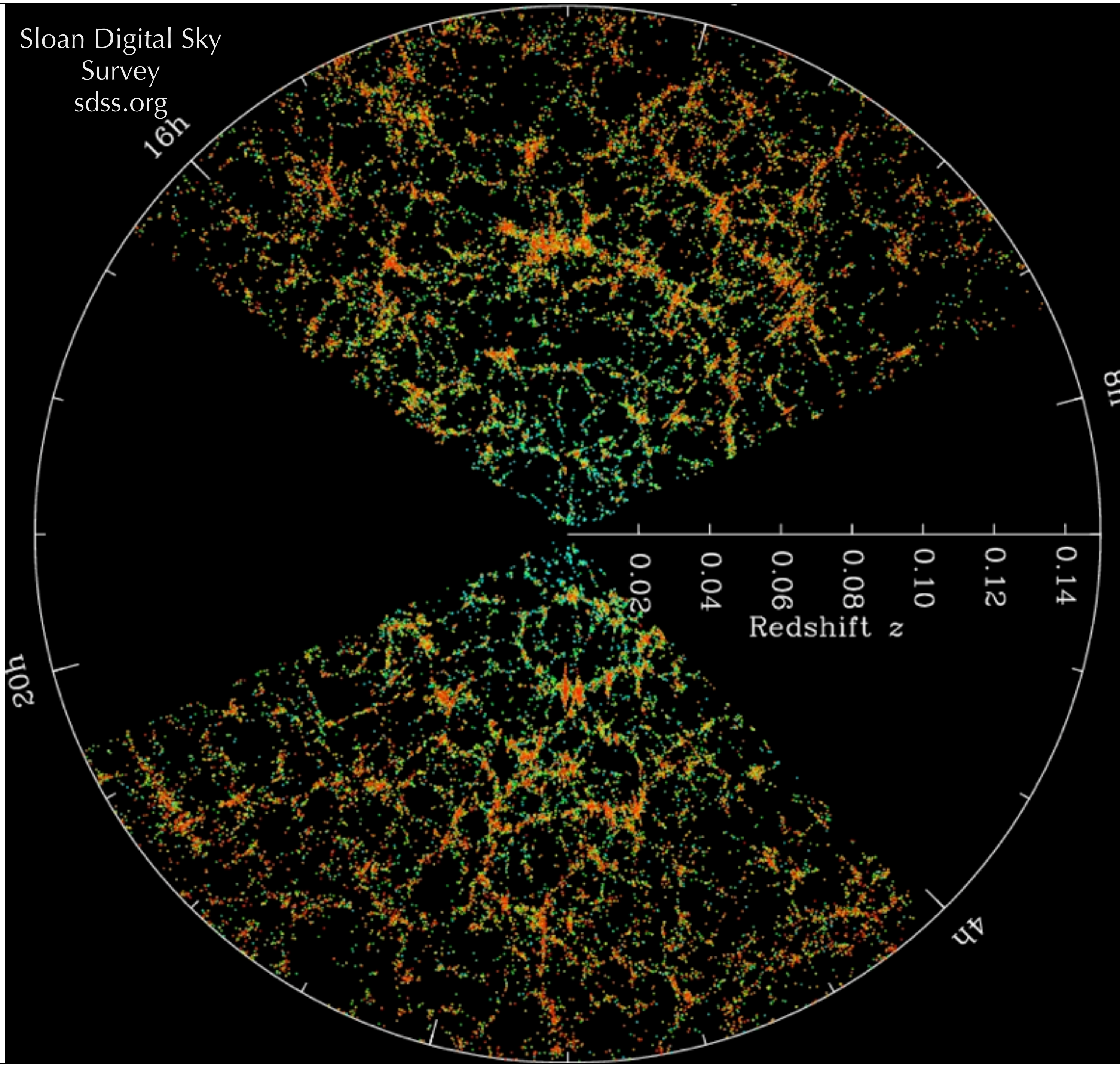
Sloan Digital Sky
Survey
sdss.org
16h
8h
20h
4h
0.02
0.04
0.06
0.08
0.10
0.12
0.14
Redshift z

galaxy catalogs from large simulations statistically match reality

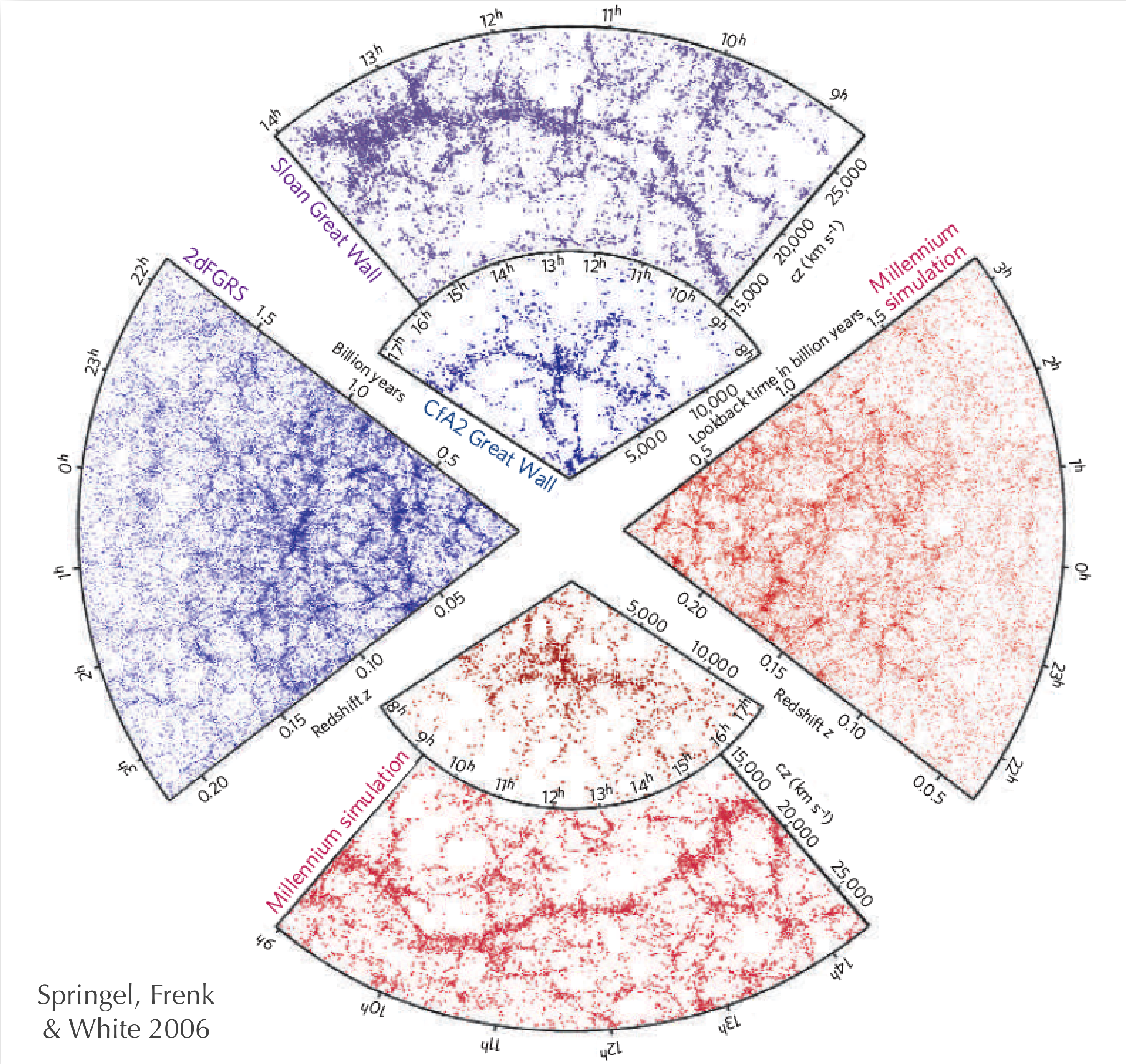

synthetic galaxy catalogs evolved from an initial random noise state with initial power spectrum dictated by CMB

an engineer's view of galaxy formation

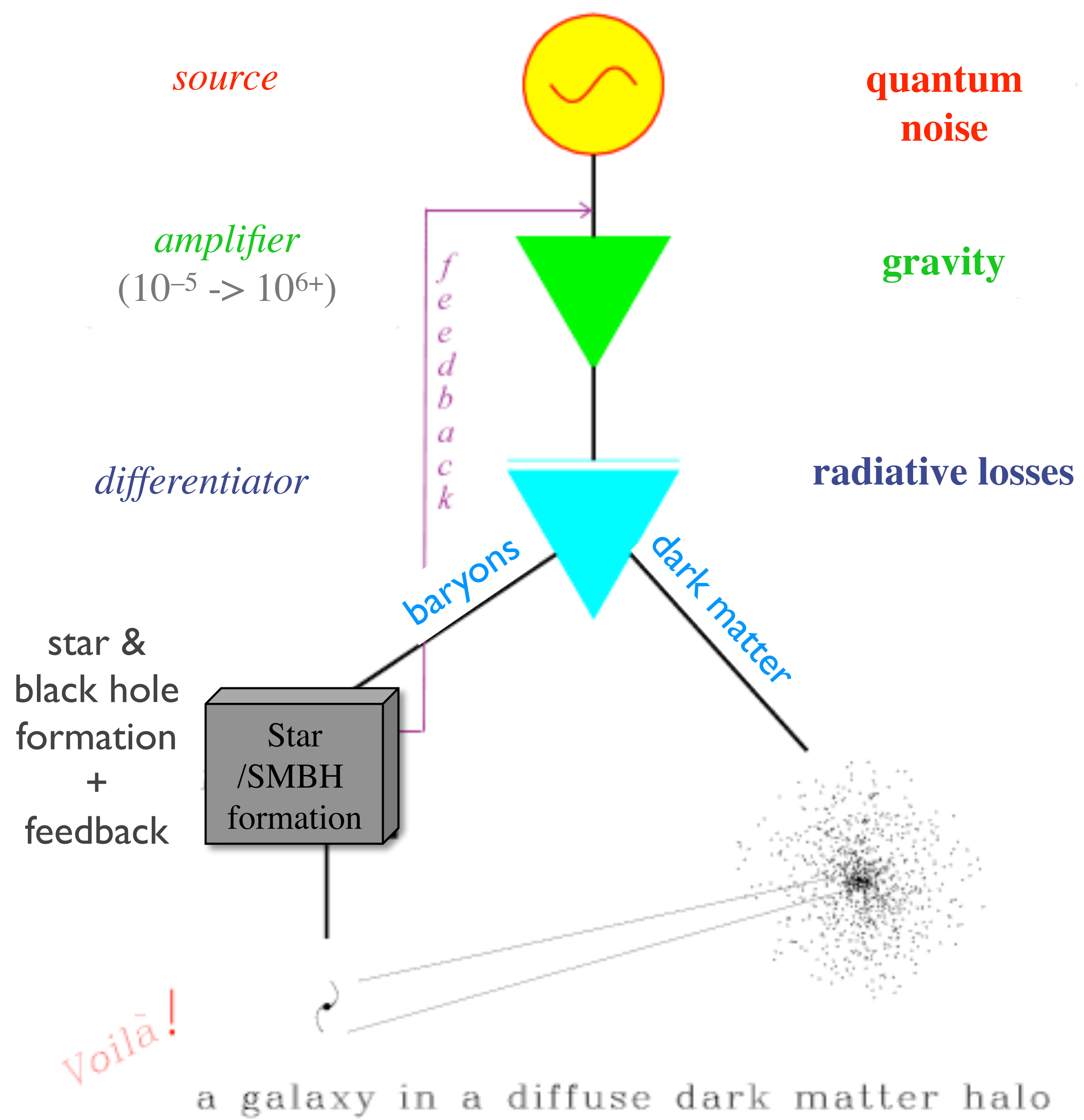

what are clusters of galaxies?

* terminus of clustering hierarchy => largest, non-linear structures

easily visible **we can find all the biggest ones now**

* multi-component - DM: hot gas: galaxies+stars :: ~100: 10: 1

many observational channels **radio/mm - IR/optical - X-ray**

* quasi-equilibrium (`frustrated') dynamical systems

~one-parameter family **tight mass-observable scalings**

LSS Simulations

THE A RNAL

AN D

VOLUME 94 NUMBER 3

ON THE EBULAE

II. A STU ODELS OF
STELI DURE

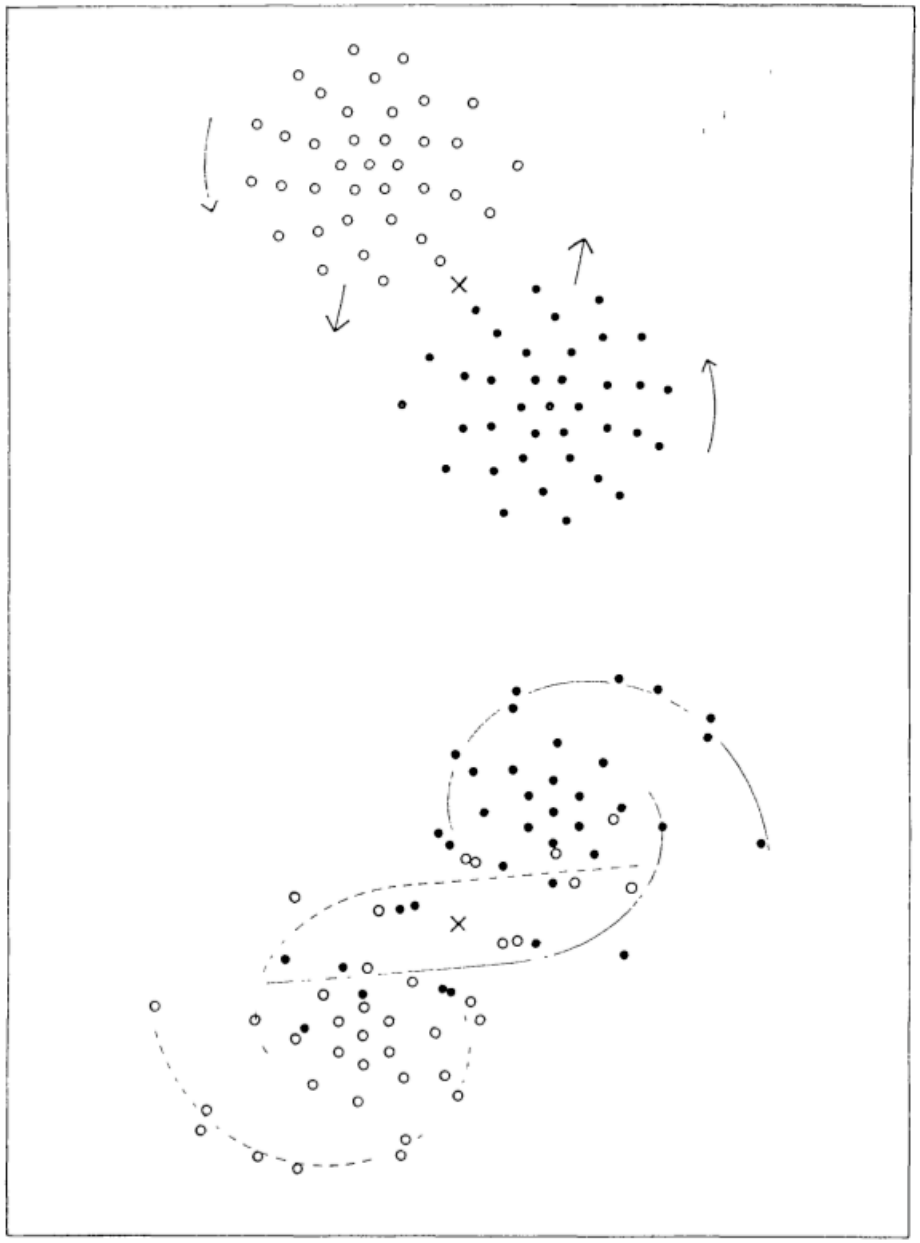

Fig. 4b

key characteristics of LSS

* galaxies and clusters of galaxies are **weak-field** structures in the expanding FRW metric,

$$v^2 / c^2 << 1$$

=> a **Newtonian** description of the gravitational potential is accurate to model the dynamics of sub-horizon LSS formation.

LSS simulations use Newtonian potential of perturbations in an expanding FRW metric.

large-scale structure simulations: methodologies

* DM evolution using collisionless N-body simulations (single fluid)

- assumes DM is weakly interacting massive particle (WIMP)
- initial density fluctuations assumed to be Gaussian random field with power spectrum, P(k), calculable from linear theory
- growing mode from linear perturbation theory sets initial conditions
- `particles' represent coarse-grained phase space kinematics
- `softening' of pair-wise force required to regularize dynamics
- individual timesteps improve performance
- Layzer-Irving equation benchmarks energy conservation (+ p,L cons.)

* coupled N-body + gas dynamics simulations (multiple fluids)

- on galactic and larger scales, baryons trace DM at high-z
- baryons are collisional, so intersecting streams generate shocks
- shocks generate thermal energy and entropy
- radiation field can produce cooling or heating in gas
- star formation prescriptions are empirically motivated

large-scale structure simulations: overview of algorithmic evolution

1960's+70's - direct (NxN) force summation

studies of galaxy encounters and stellar clusters

1980's - particle-mesh (FFT's) and Tree algorithms for large-scale gravity

studies of `cosmic web' topology from initial random noise field

1990's - parallelization on Beowulf clusters, special purpose chips (GRAPE)

detailed studies of clustering statistics, cosmological dependence

- first multi-fluid codes to model coupled dark matter and baryons

initial studies of galaxy formation

2000's - massive parallelization on large-scale supercomputers

toward precision calibrations of large-scale structure statistics

- multi-fluid codes with approx. radiation transfer, MHD

initial studies of stellar feedback effects, high-rez galaxy formation

Supercomputing Ecosystem (2005)

courtesy Horst Simon (LBL)

Commercial Off The Shelf technology (COTS)

"Clusters"

12 years of legacy MPI applications base

From my presentation at ISC 2005

Traditional Sources of Performance Improvement are Flat-Lining (2004)

- **New Constraints**
  - 15 years of *exponential* clock rate growth has ended
- **Moore's Law reinterpreted:**
  - How do we use all of those transistors to keep performance increasing at historical rates?
  - Industry Response: #cores per chip doubles every 18 months *instead* of clock frequency!

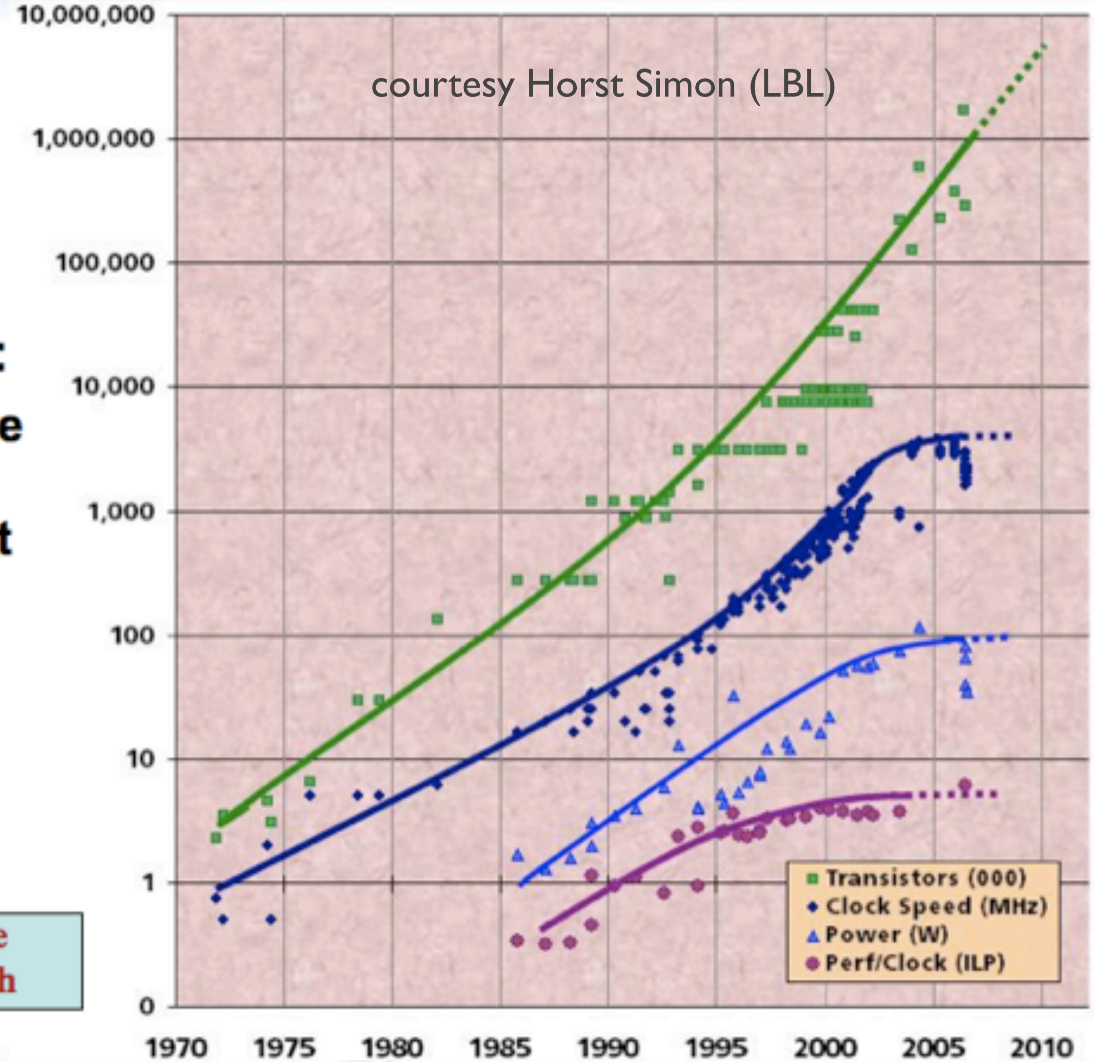

Figure courtesy of Kunle Olukotun, Lance Hammond, Herb Sutter, and Burton Smith

BERKELEY LAB

U.S. DEPARTMENT OF ENERGY

Office of Science

TOP500 SUPERCOMPUTER SITES

Performance Projection

courtesy Horst Simon (LBL)

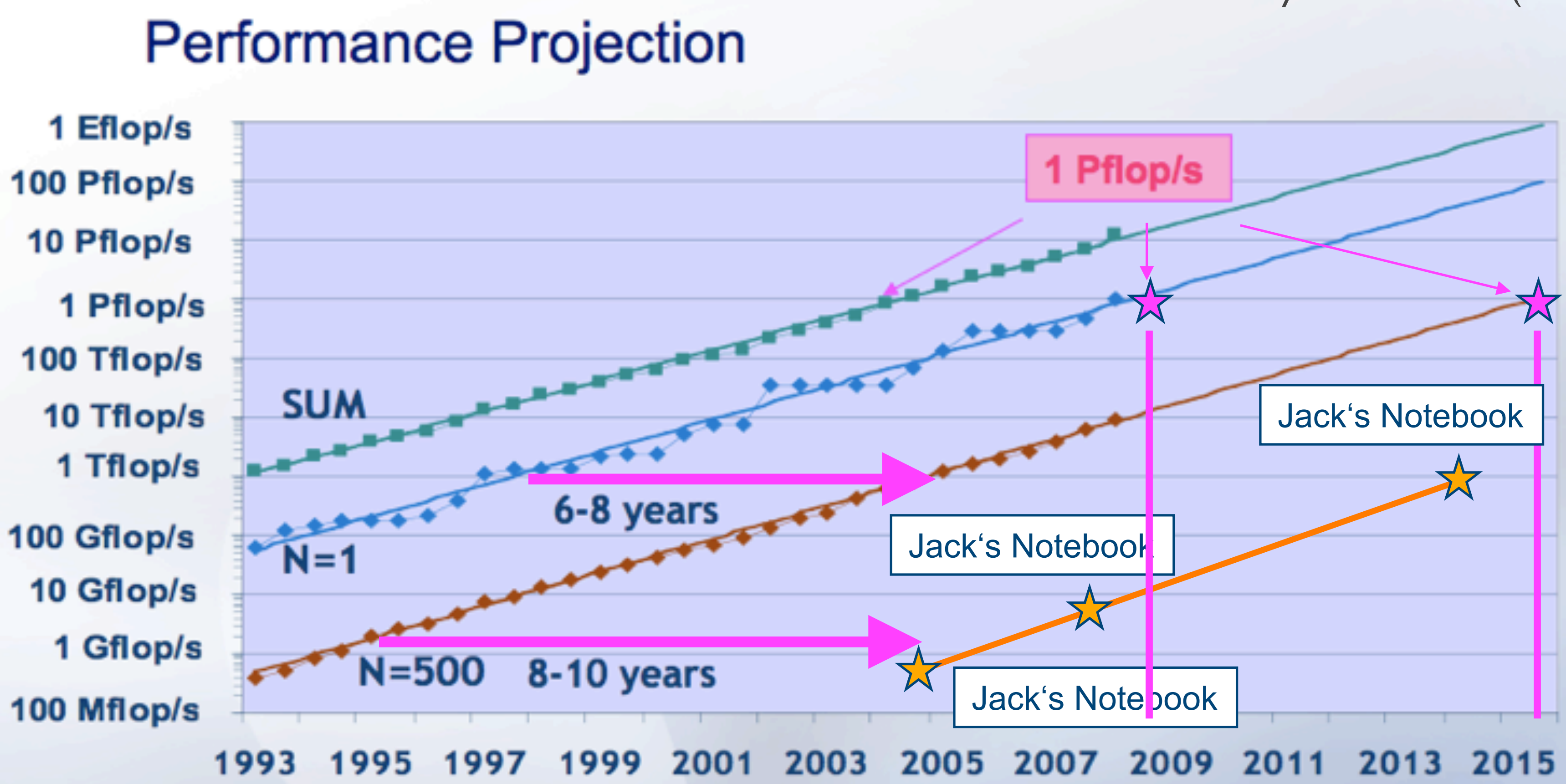

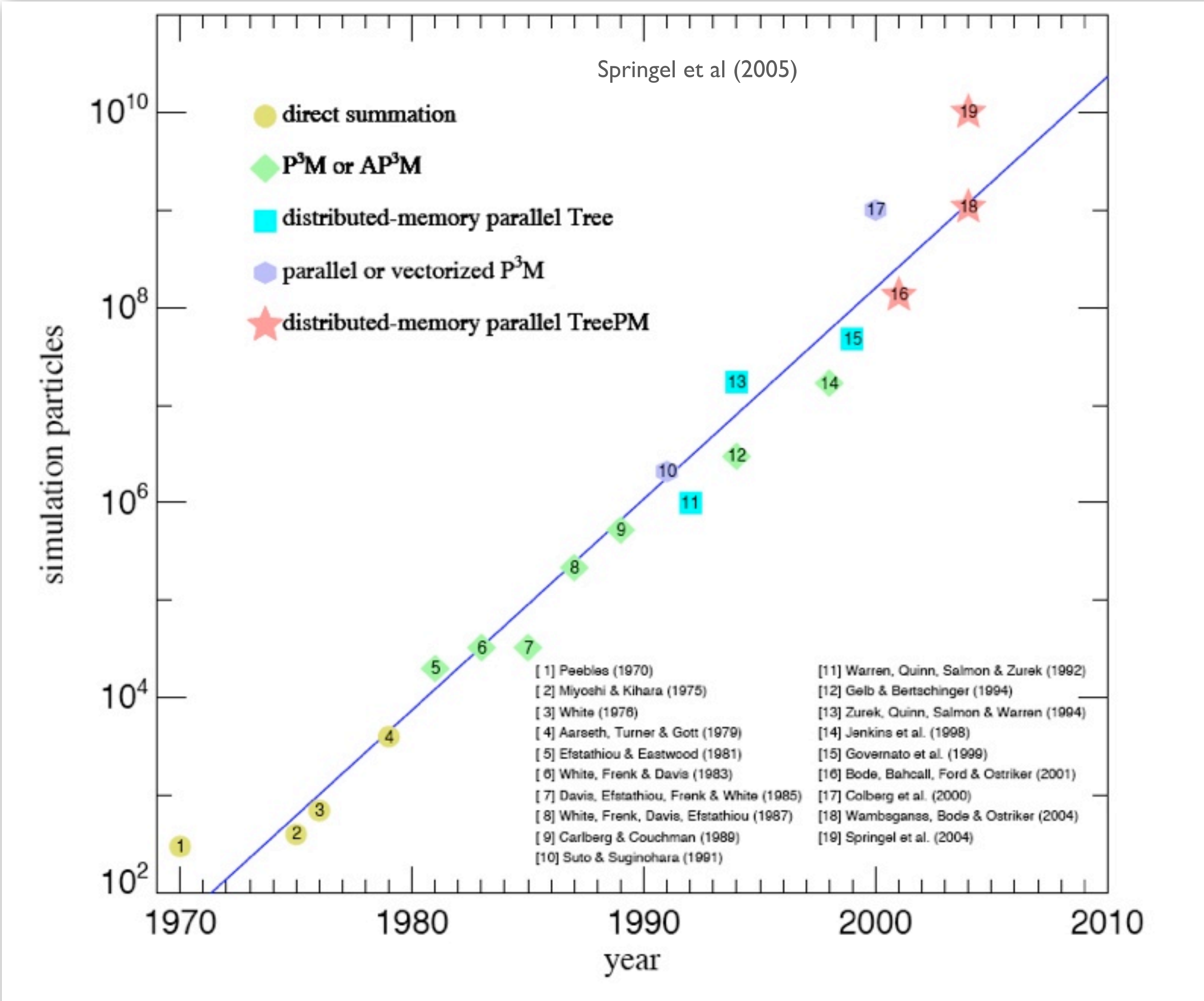

Springel et al (2005)
direct summation
P³M or AP³M
distributed-memory parallel Tree
parallel or vectorized P³M
distributed-memory parallel TreePM
simulation particles
year
[1] Peebles (1970)
[2] Miyoshi & Kihara (1975)
[3] White (1976)
[4] Aarseth, Turner & Gott (1979)
[5] Efstathiou & Eastwood (1981)
[6] White, Frenk & Davis (1983)
[7] Davis, Efstathiou, Frenk & White (1985)
[8] White, Frenk, Davis, Efstathiou (1987)
[9] Carlberg & Couchman (1989)
[10] Suto & Suginohara (1991)
[11] Warren, Quinn, Salmon & Zurek (1992)
[12] Gelb & Bertschinger (1994)
[13] Zurek, Quinn, Salmon & Warren (1994)
[14] Jenkins et al. (1998)
[15] Governato et al. (1999)
[16] Bode, Bahcall, Ford & Ostriker (2001)
[17] Colberg et al. (2000)
[18] Wambsganss, Bode & Ostriker (2004)
[19] Springel et al. (2004)

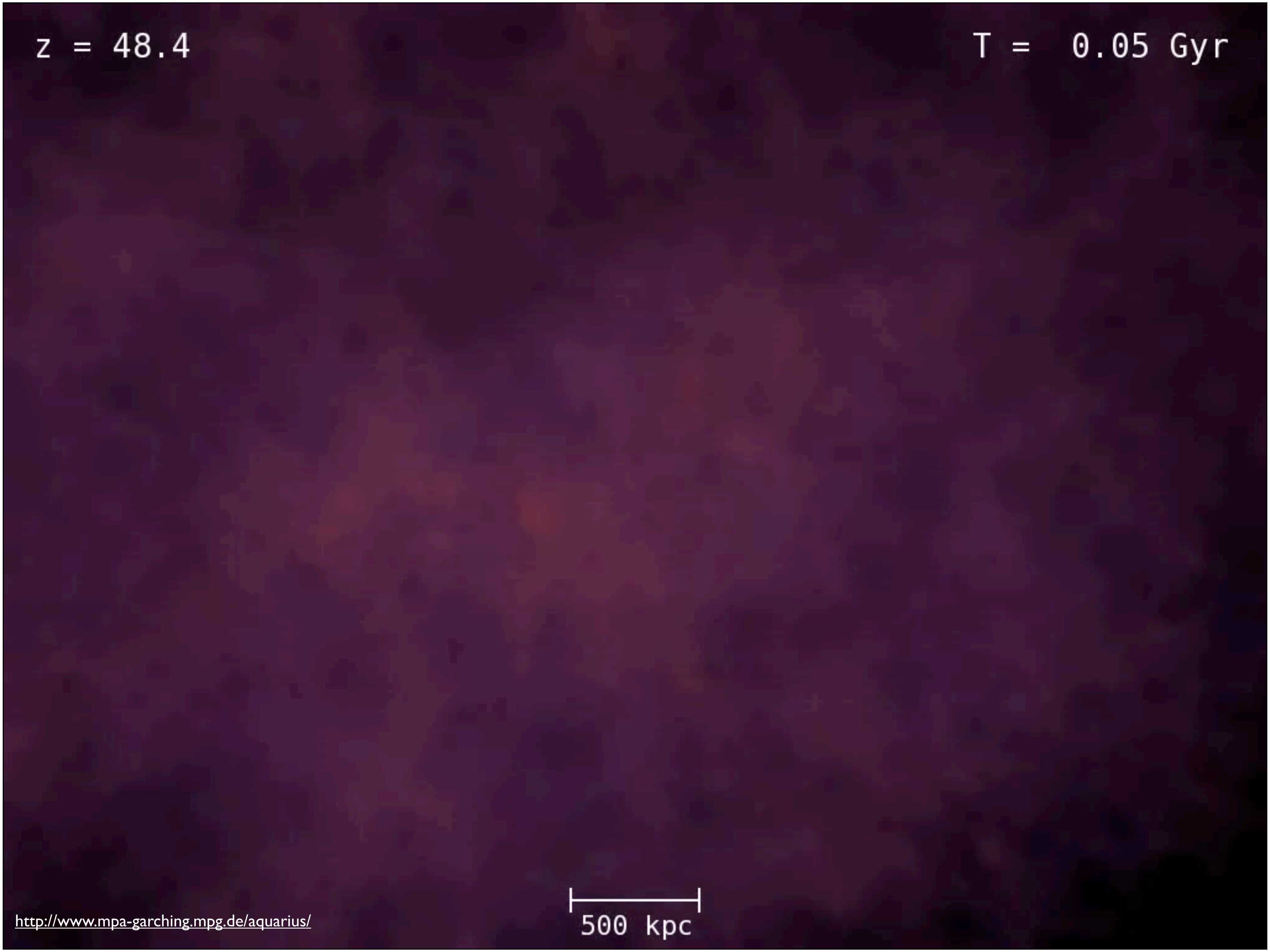

http://www.mpa-garching.mpg.de/aquarius/

LSS is a ***cosmic web*** connecting locally bound structures called ***halos***

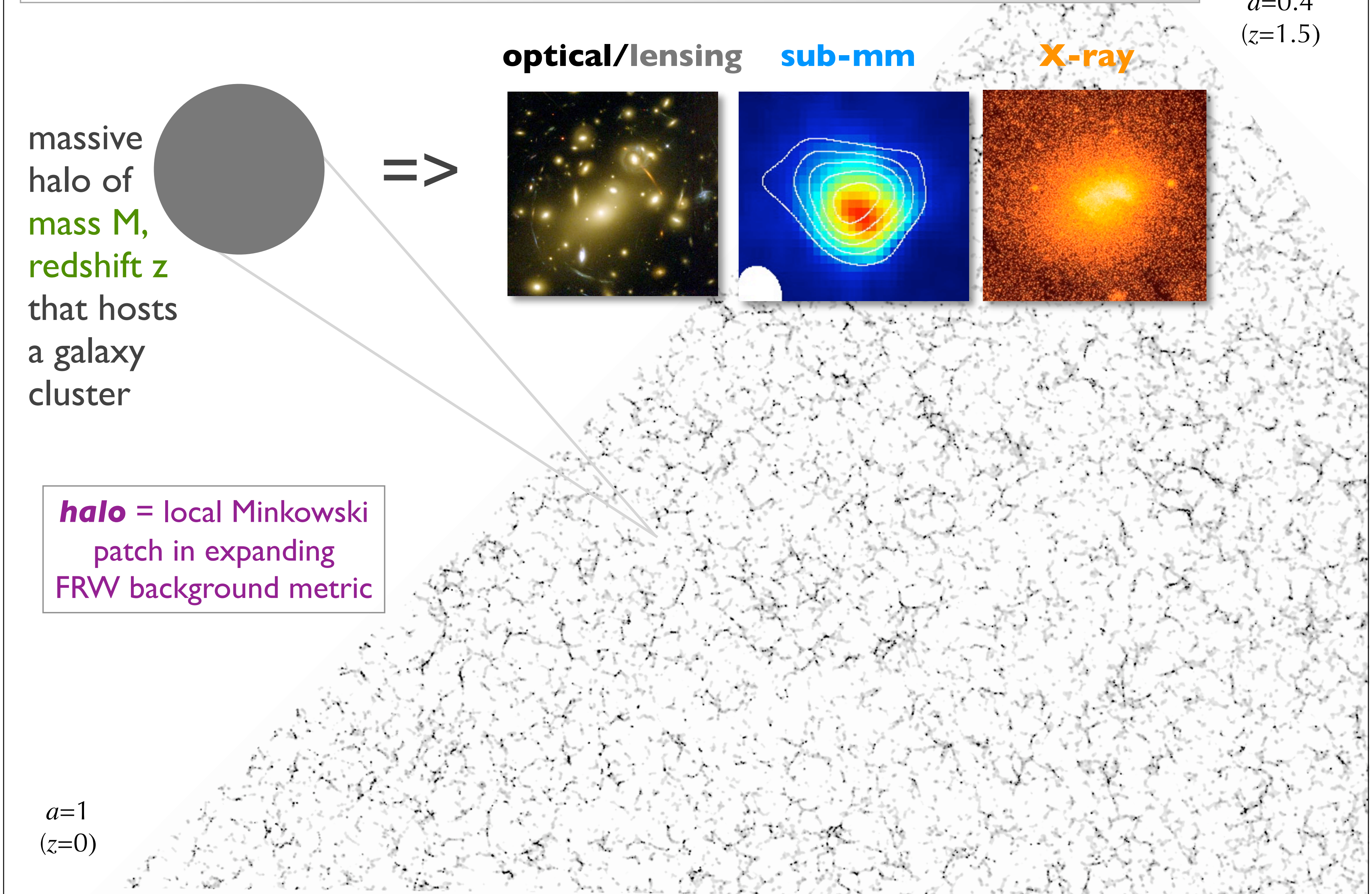

collisionless N-body: applications to dark matter evolution

* single halo simulations to study
  - substructure (sub^N-halos)
  - direct dark matter detection signatures
  - faint galaxy luminosity function

    + ...

* cosmological volumes to study
  - halo space density (aka, ***mass function***)
  - halo clustering (aka, ***bias***)

    + ...

* large ensemble of runs to study
  - precise evolution of non-linear power spectrum, $P(k)$

    LANL+Argonne emulation campaign (Heitmann, Habib+)
  - covariance of LSS signatures (lensing, clustering, +)

cosmological N-body systems

* model triply-periodic cube in comoving frame
  (infinite volume of cubic replications)

Efstathiou et al 1985
Bertschinger 1998
Springel et al 2001
Springel 2005

* `peculiar' (non-Hubble) particle equation of motion

Dark matter is represented in cosmological simulations by particles sampling the phase space distribution. Particles are evolved forward in time using Newton's laws written in comoving coordinates (Peebles 1980):

$$\frac{d\vec{x}}{dt} = \frac{1}{a}\vec{v}, \quad \frac{d\vec{v}}{dt} + H\vec{v} = \vec{g}, \quad \vec{\nabla} \cdot \vec{g} = -4\pi G a[\rho(\vec{x}, t) - \bar{\rho}(t)]. \tag{1}$$

Here $a(t)$ is the cosmic expansion factor (related to redshift z by $a^{-1} = 1 + z$), $H = d \ln a/dt$ is the Hubble parameter, $\vec{v}$ is the peculiar velocity, ρ is the mass density, $\bar{\rho}$ is the spatial mean density, and $\vec{\nabla} = \partial/\partial\vec{x}$ is the gradient in comoving coordinates. Note that the first pair of relationships in Equation 1 is to be integrated for every dark matter particle by using the gravity field produced by all matter (dark and baryonic) contributing to ρ.

Bertschinger 1998

cosmological N-body systems: various methods to compute acceleration

Bertschinger 1998

TREE: The hierarchical tree algorithm (Appel 1985, Barnes & Hut 1986) divides space recursively into a hierarchy of cells, each containing one or more particles. When computing the gravitational acceleration of a particle, a cell of size s a distance d from that particle is treated as one pseudoparticle (located at the center of mass of the cell) if the cell satisfies a critical ***non-opening condition***, $s/d < \theta$. Otherwise, the cell is `opened' and to the a higher level in the hierarchy and the condition tested again. Computation is thus saved by replacing the set of particles by a low-order multipole expansion due to the distribution of mass in the cell.

PARTICLE-MESH: The particle-mesh (PM) method is based on representing the gravitational potential on a Cartesian grid (with a total of N_g grid points), used in solving Poisson's equation on this grid. The development of the Fast Fourier Transform (FFT) algorithm (Cooley & Tukey 1965) made possible a fast Poisson solver requiring $O(N_g \log N_g)$ operations (Miller & Prendergast 1968, Hohl & Hockney 1969, Miller 1970).

The PM algorithm has three basic steps:

1) The particles are `assigned' to nearby grid points to create a density field on the grid. This is then FFT'ed to create a Fourier representation of the density field.

2) Poisson's equation is solved in Fourier space.

$$\hat{\phi}(\vec{k}, t) = -4\pi G a^2 \frac{\hat{\rho}(\vec{k}, t)}{k^2}.$$

3) The gravity field (or the potential, which is then differenced to give the gravity field) is determined on the grid, and interpolated back to determine particle acceleration.

cosmological N-body systems: various methods (cont'd)

Bertschinger 1998

PP-PM (P3M): This hybrid algorithm, first developed for plasma physics by Hockney et al (1974), was applied in cosmology by Efstathiou & Eastwood (1981). It is described in detail by Hockney & Eastwood (1988) and Efstathiou et al (1985), and it was used extensively by the latter authors in a series of articles beginning with Davis et al (1985).
The P3M method readily achieves high accuracy forces through the combination of mesh-based and direct summation forces. The mesh may be regarded as simply a convenience for providing periodic boundary conditions and removing much of the burden of computation from the direct pair summation.

The short-range calculation computes the difference between Newtonian gravity and the grid force, stored as a look-up table as a function of r, within a sphere of radius ~3 grid cells.

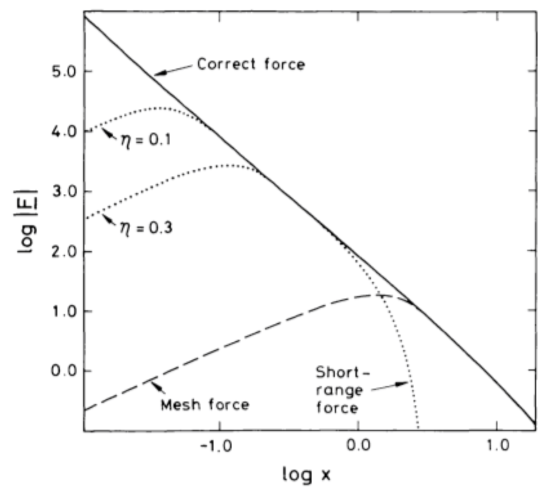

TREE-PM: Similar to P3M, but the short-range force is computed by a tree algorithm rather than direct particle summation. The **gadget** code, developed by Volker Springel and colleagues, is a popular TREE-PM that represents state-of-the-art in N-body cosmological methods.

http://www.mpa-garching.mpg.de/gadget/

cosmological N-body systems: evolving the system

Efstathiou et al 1985

* time evolution is typically 2nd-order accurate (e.g., leapfrog)

In comoving coordinates, Newton's equations of motion are (see, e.g., Peebles 1980, § 7),

$$\dot{\boldsymbol{v}}_i + 2\frac{\dot{a}}{a}\boldsymbol{v}_i = -a^{-3}\sum_{i \neq j}\frac{Gm_j\boldsymbol{x}_{ij}}{|\boldsymbol{x}_{ij}|^3} = a^{-3}\boldsymbol{F}_i/m_i, \tag{9}$$

where m_i is the mass of the ith particle, dots denote differentiation with respect to time, and $\boldsymbol{v} = \dot{\boldsymbol{x}}$. To integrate equation (9) numerically, it is convenient to transform to a new time variable $p = a^\alpha$. Equation (9) then becomes

$$\frac{d\boldsymbol{u}_i}{dp} + 2A(p)\boldsymbol{u}_i = B(p)\boldsymbol{F}_i/m_i, \tag{10a}$$

where

$$\boldsymbol{u} = \frac{d\boldsymbol{x}}{dp}, \quad A(p) = \frac{(1+\alpha+\ddot{a}a/\dot{a}^2)}{2\alpha a^\alpha}, \quad B(p) = \frac{1}{\alpha^2\dot{a}^2a^{2\alpha+1}}.$$

In the N-body codes described here, the positions are specified at step n and the velocities are specified at step $n-1/2$. The forces on the particles are computed using the methods described in § II, and the positions and velocities of the ith particle are incremented according to the time-centered leapfrog scheme:

$$\boldsymbol{u}_{n+1/2} = \boldsymbol{u}_{n-1/2}\frac{(1-A_n\Delta p)}{(1+A_n\Delta p)} + \frac{B_n\boldsymbol{F}_n\Delta p}{(1+A_n\Delta p)m_i}, \tag{11a}$$

$$\boldsymbol{x}_{n+1} = \boldsymbol{x}_n + \boldsymbol{u}_{n+1/2}\Delta p, \tag{11b}$$

where A_n and B_n are the values of A and B at step n and Δp is the time step. With this integration scheme, the errors in both positions and velocities are of order $(\Delta p)^3$ per time step.

* Layzer-Irvine equation for energy conservation (~0.5% typical accuracy)

$$\frac{d(a^4T)}{dt} + a\frac{dU}{dt} = 0,$$

where

$$T = \frac{1}{2}\sum_i m_i v_i^2, \quad U = \frac{1}{2}\sum_i m_i\phi_i,$$

Written in integral forms, where C and C' are constants

$$a^4T + aU - \int U da = C,$$

$$a^3T + U + \int a^2T da = C',$$

* Zel’dovich approximation (1st order linear PT):

Efstathiou et al 1985

A convenient and efficient method for setting up initial conditions with any desired power spectrum can be derived from Zel’dovich’s (1970) formulation of the linear evolution of a general distribution of fluctuations

$$\boldsymbol{x}(t) = \boldsymbol{q} - b(t)\,\psi(\boldsymbol{q}), \tag{19}$$

where $\boldsymbol{x}$ is the comoving Eulerian coordinate of a particle, $\boldsymbol{q}$ is the Lagrangian coordinate denoting its initial position, $b(t)$ is the growth factor of linear fluctuations, and ψ describes the spatial structure of the density fluctuations. Substituting this relation into the equations of motion (eq. [9]), we can express ψ in terms of the force field at time t,

$$\psi(\boldsymbol{q}) = -\frac{\boldsymbol{F}(\boldsymbol{q},t)}{ma^2(a\ddot{b} + 2\dot{b}\dot{a})}. \tag{20}$$

$$\dot{\boldsymbol{x}} = -\dot{b}\,\psi(\boldsymbol{q}). \tag{21}$$

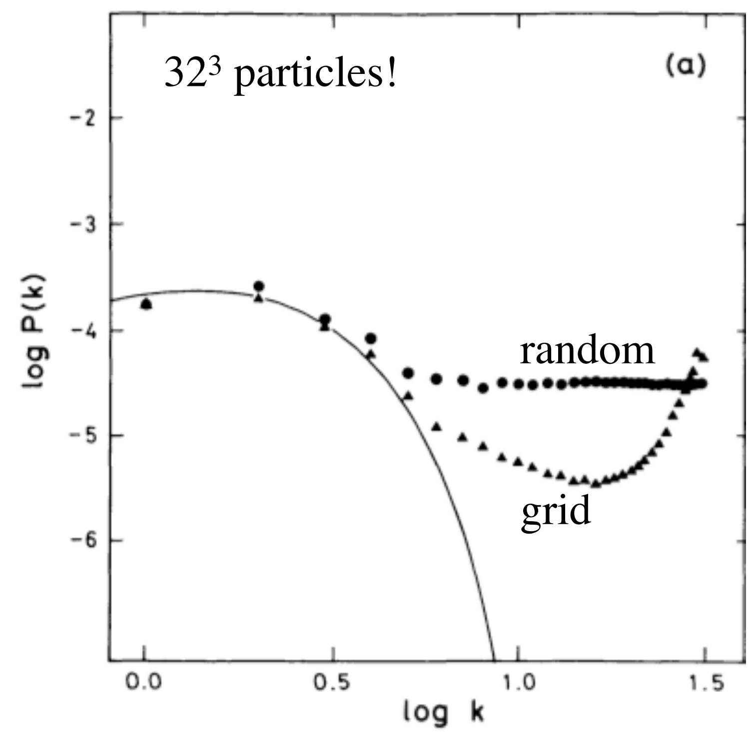

initial conditions: next order to suppress non-growing mode transients

* 2LPT (2nd-order linear PT):

Crocce, Pueblas, Scoccimarro (2006)

The equations of motion for the evolution of dark matter can be written in a compact way by introducing the two-component 'vector'

$$\Psi_a(\boldsymbol{k}, \eta) \equiv (\delta(\boldsymbol{k}, \eta), \ -\theta(\boldsymbol{k}, \eta)/\mathcal{H}), \tag{1}$$

where the index $a = 1, 2$ selects the density or velocity components, with $\delta(\boldsymbol{k})$ being the Fourier transform of the density contrast $\delta(\boldsymbol{x}, \tau) = \rho(\boldsymbol{x})/\bar{\rho} - 1$ and similarly for the peculiar velocity divergence $\theta \equiv \nabla\cdot\boldsymbol{v}$. $\mathcal{H} \equiv \mathrm{d}\ln a/\mathrm{d}\tau$ is the conformal expansion rate with $a(\tau)$ being the cosmological scale factor and τ being the conformal time. The time variable η is defined from the scale factor by

$$\eta \equiv \ln a(\tau), \tag{2}$$

$$\boxed{\begin{aligned}\Psi_a(\boldsymbol{k}, \eta) = g_{ab}(\eta)\,\phi_b(\boldsymbol{k}) + \int_0^{\eta} \mathrm{d}\eta'\ g_{ab}(\eta - \eta') \\ \times \gamma^{(s)}_{bcd}(\boldsymbol{k}, \boldsymbol{k}_1, \boldsymbol{k}_2)\Psi_c(\boldsymbol{k}_1, \eta')\Psi_d(\boldsymbol{k}_2, \eta'),\end{aligned}} \tag{7}$$

$$g_{ab}(\eta) = \frac{e^{\eta}}{5}\begin{bmatrix} 3 & 2 \\ 3 & 2 \end{bmatrix} - \frac{e^{-3\eta/2}}{5}\begin{bmatrix} -2 & 2 \\ 3 & -3 \end{bmatrix}. \tag{9}$$

$$\gamma^{(s)}_{121}(\boldsymbol{k}, \boldsymbol{k}_1, \boldsymbol{k}_2) = \delta_{\mathrm{D}}(\boldsymbol{k} - \boldsymbol{k}_1 - \boldsymbol{k}_2)\,\frac{(\boldsymbol{k}_1 + \boldsymbol{k}_2)\cdot\boldsymbol{k}_1}{2k_1^2}, \tag{5}$$

$$\gamma^{(s)}_{222}(\boldsymbol{k}, \boldsymbol{k}_1, \boldsymbol{k}_2) = \delta_{\mathrm{D}}(\boldsymbol{k} - \boldsymbol{k}_1 - \boldsymbol{k}_2)\,\frac{|\boldsymbol{k}_1 + \boldsymbol{k}_2|^2(\boldsymbol{k}_1\cdot\boldsymbol{k}_2)}{2k_1^2k_2^2}, \tag{6}$$

$\gamma^{(s)}_{abc}(\boldsymbol{k}, \boldsymbol{k}_i, \boldsymbol{k}_j) = \gamma^{(s)}_{acb}(\boldsymbol{k}, \boldsymbol{k}_j, \boldsymbol{k}_i)$ and γ is zero otherwise, δ_{D} denotes the Dirac delta distribution. The formal integral solution to equa-

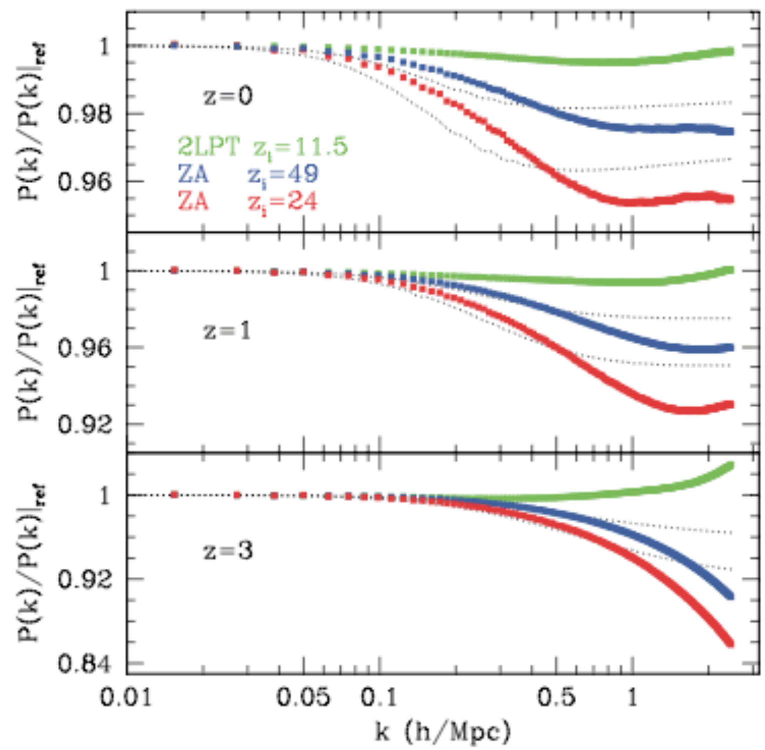

Figure 6. Power spectrum for different initial conditions (2LPT $z_i = 11.5$, ZA $z_i = 49$ and ZA $z_i = 24$, from top to bottom in each panel) compared to the reference runs at $z = 0$ (top), $z = 1$ (middle) and $z = 3$ (bottom). The dotted lines show an estimate of the transients for ZA $z_i = 49$ and ZA $z_i = 24$ from one-loop PT.

force softening: mass and spatial resolution

* discreteness imposes
- finite particle mass
- softening of potential at small r (to avoid infinite forces at r=0)

* various studies of how best to set these parameters, but in practice

$$m_p = \rho_m L^3 / N_p$$
$$\text{soft} \sim (0.1\text{-}0.2)\ L / N_p^{1/3}$$

Convergence tests are a pragmatic approach to testing discreteness effects

Steinmetz and White (1997)

Consider a fluid element of mass m_g and density ϱ_g which is at rest. This fluid element encounters a dark matter particle of mass $M_{\rm DM}$ and relative velocity v with a closest approach distance b. In the impulse approximation (see, e.g., Binney & Tremaine 1987), the fluid element is accelerated to velocity

$$\Delta v = \frac{2\,G\,M_{\rm DM}}{b\,v}\,, \tag{1}$$

or to a corresponding kinetic energy

$$\Delta E = \frac{2\,G^2\,M_{\rm DM}^2\,m_g}{b^2\,v^2}\,. \tag{2}$$

This energy is dissipated to heat by shocks, by artificial viscosity, or by an adiabatic expansion of the gas to a new equilibrium state. Such encounters occur with a rate $2\pi\,v\,b\,{\rm d}b\,\varrho_{\rm DM}M_{\rm DM}^{-1}$, so the heating rate can be written as

$$\left.\frac{{\rm d}E}{{\rm d}t}\right|_{\rm heat} = \int {\rm d}^3v\, f(v) \int_{b_{\rm min}}^{b_{\rm max}} 2\,\pi\,{\rm d}b\, \frac{2\,G^2\,M_{\rm DM}\,\varrho_{\rm DM} m_g}{b\,v}\,, \tag{3}$$

where $f(v)$ is the velocity distribution function for the dark matter particles. Assuming this to be Maxwellian, we obtain, after the evaluation of the integrals,

$$\left.\frac{{\rm d}E}{{\rm d}t}\right|_{\rm heat} = \sqrt{\frac{32\,\pi}{3}}\,G^2\,\ln\Lambda\,\frac{M_{\rm DM}\,m_g\,\varrho_{\rm DM}}{\sigma_{\rm 1D}}\,, \tag{4}$$

$\sigma_{\rm 1D}$ being the 1D velocity dispersion of the dark matter and $\ln\Lambda$ the Coulomb logarithm. For typical galaxy formation experiments $\ln\Lambda$ is in the range 3 to 7.

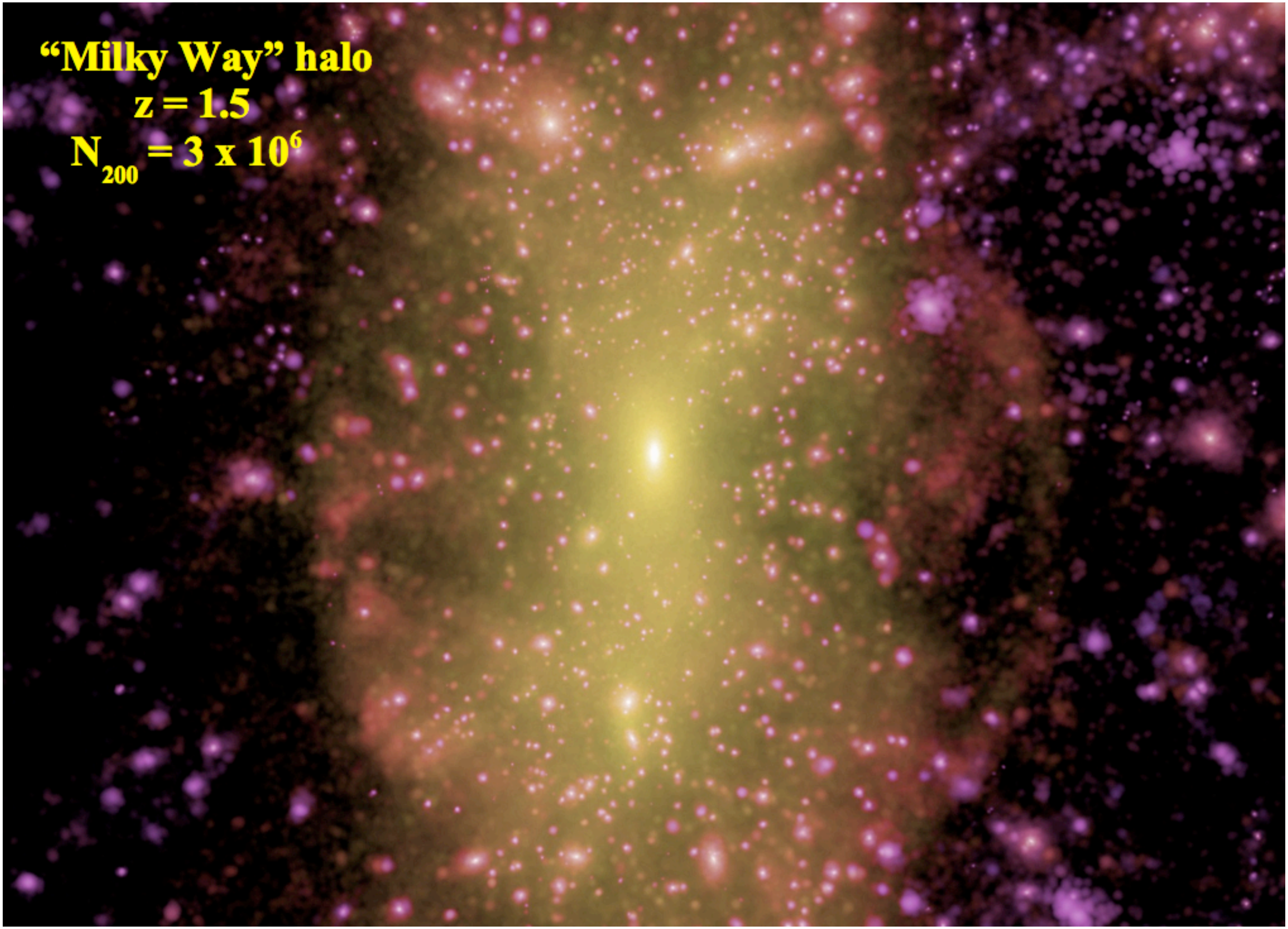

courtesy S.D.M. White, CATB2009

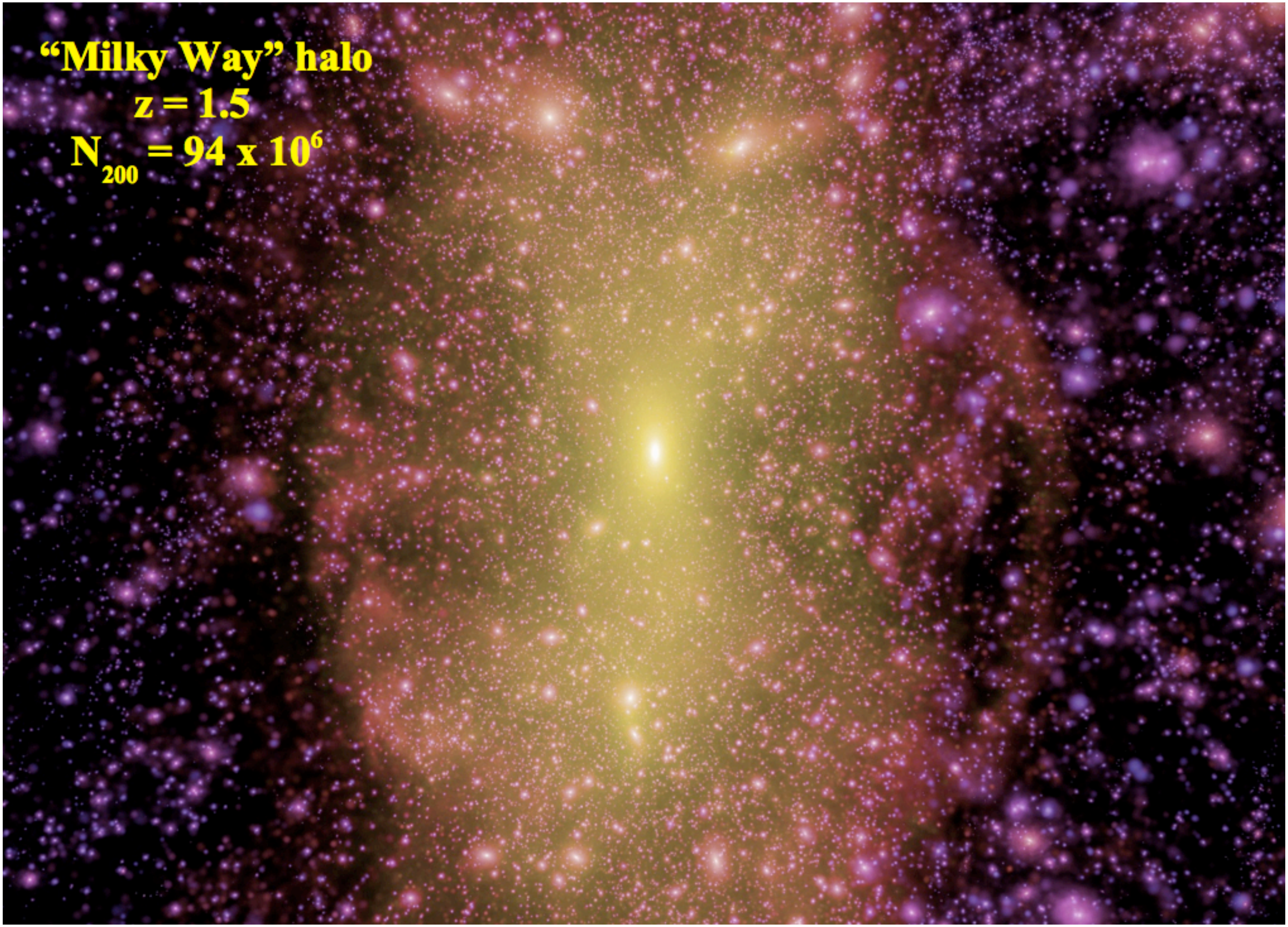

courtesy S.D.M. White, CATB2009

courtesy S.D.M. White, CATB2009

Position Space @ 8 kpc

M. Zemp
Via Lactea II

|v|

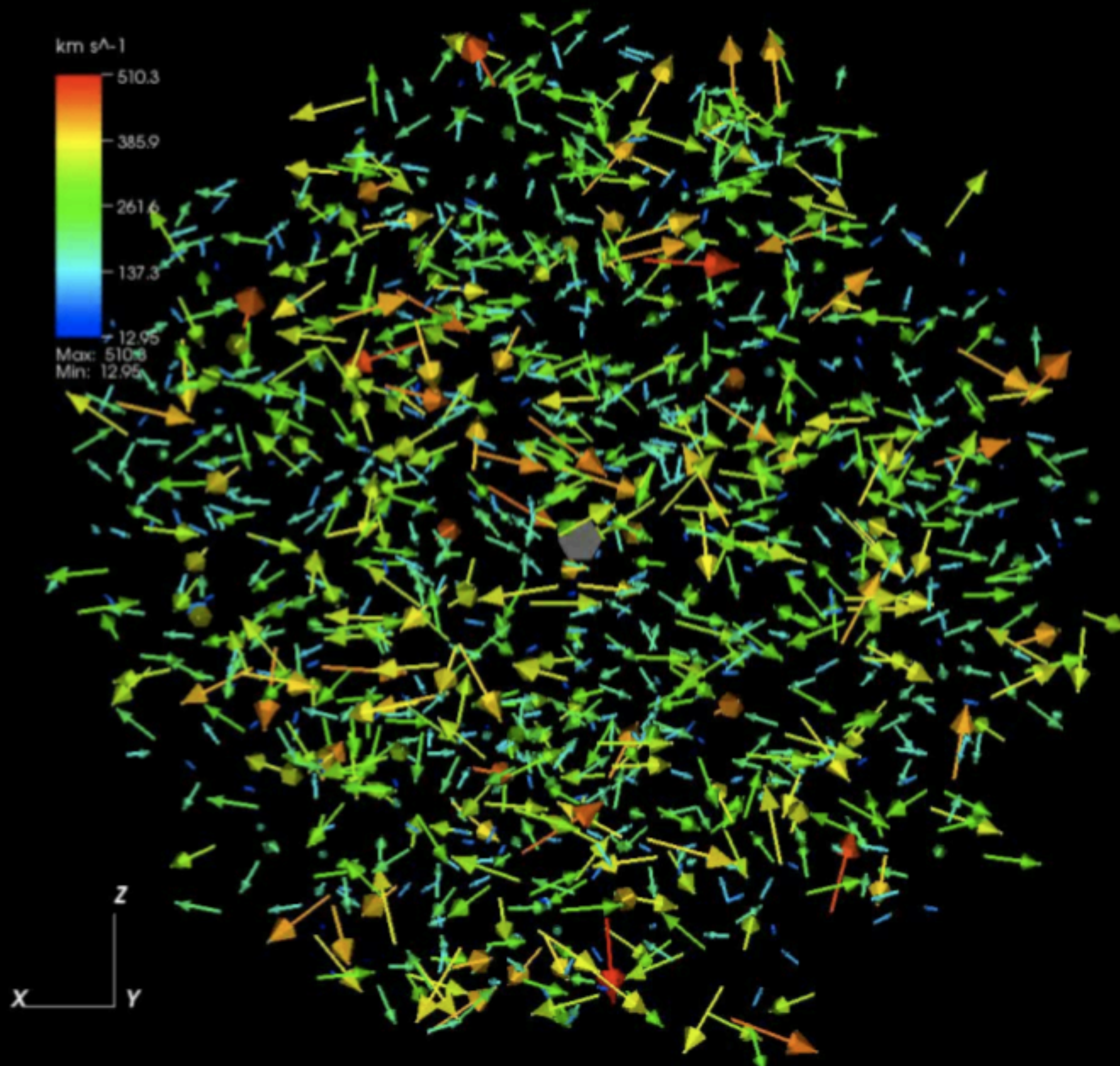

r = (0,8,0) kpc
d = 1 kpc

Velocity Space @ 8 kpc

M. Zemp
Via Lactea II

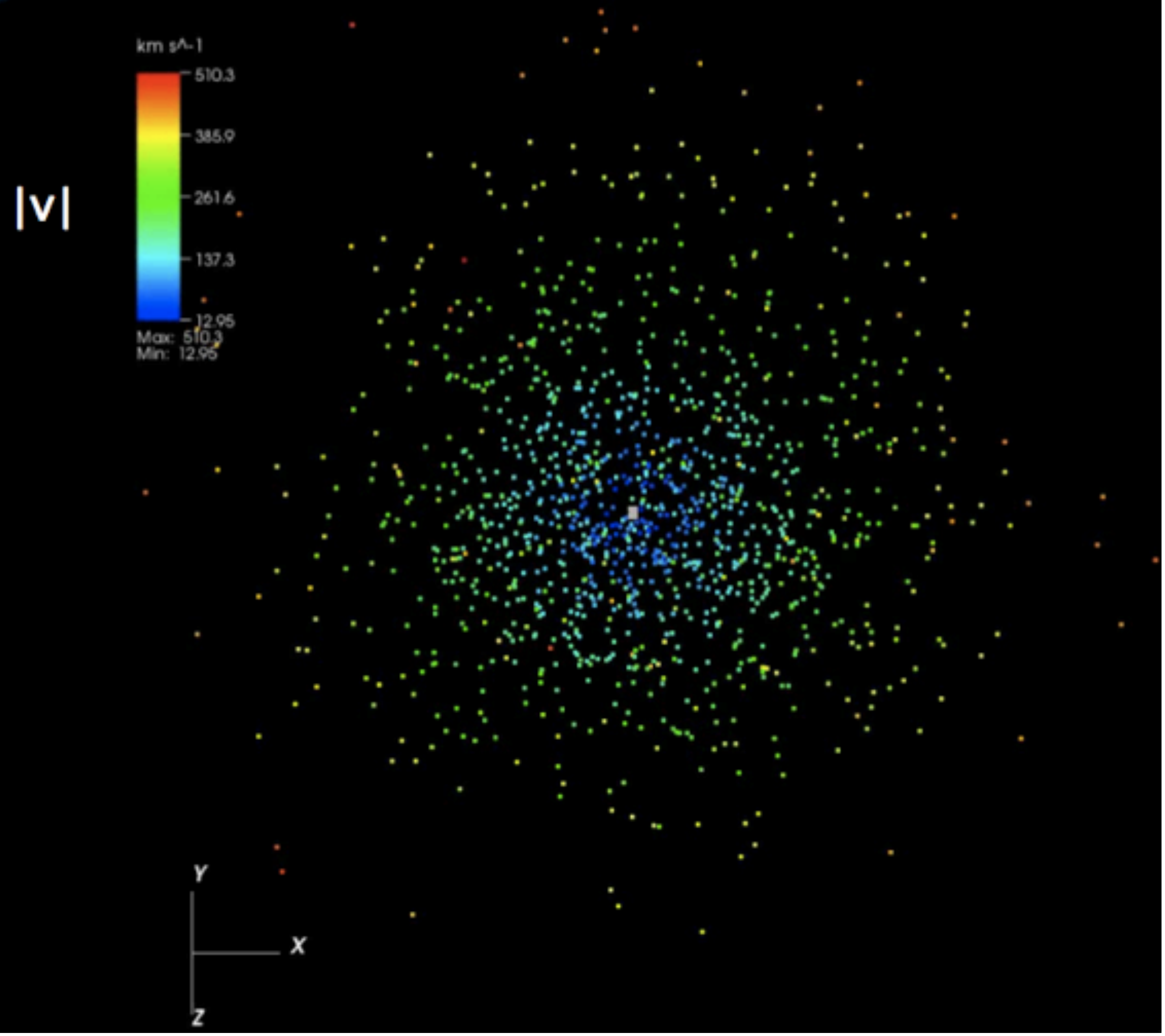

r = (0,8,0) kpc
d = 1 kpc

Position Space @ 400 kpc

M. Zemp
Via Lactea II

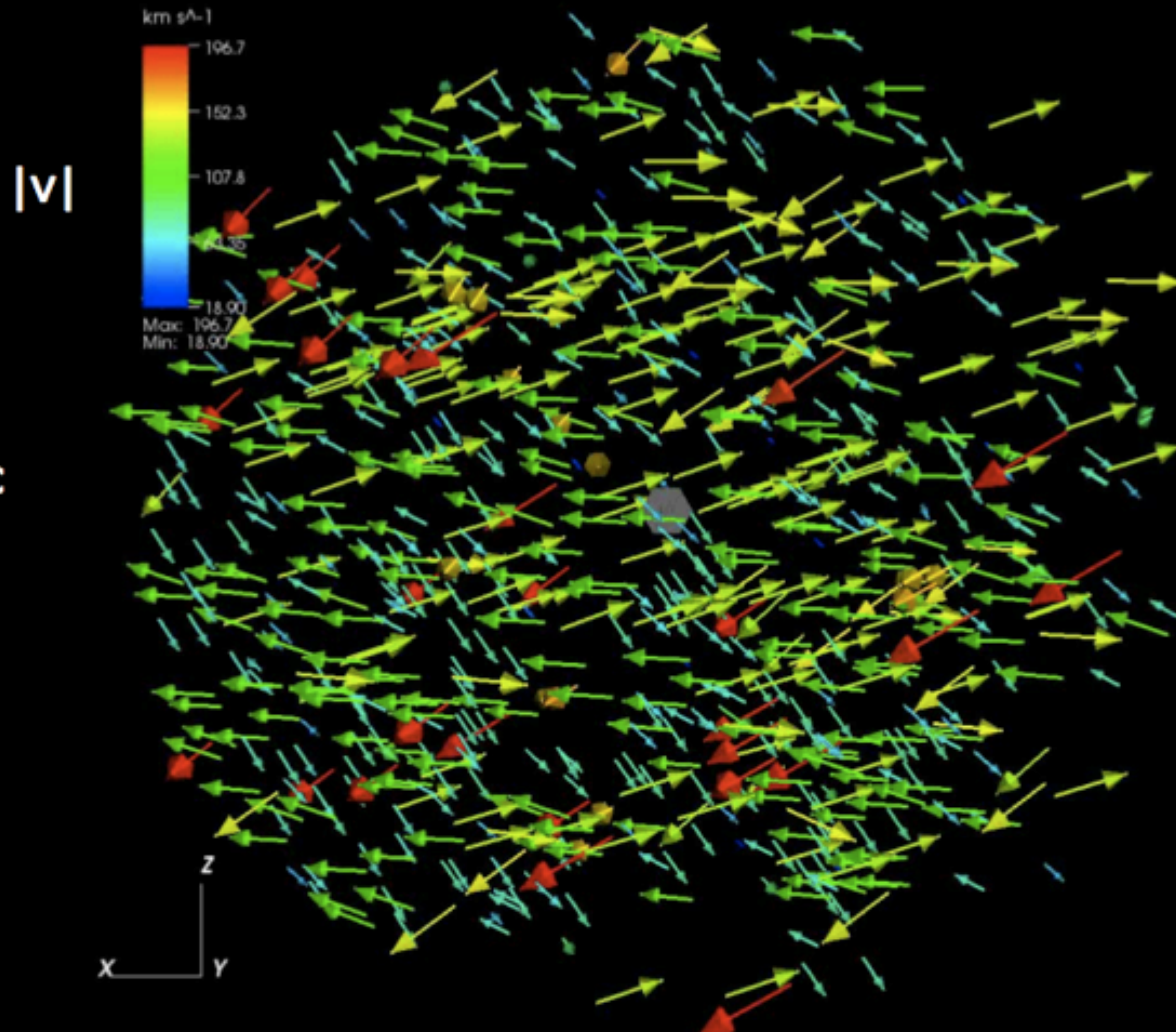

r = (0,400,0) kpc
d = 21.4 kpc

Velocity Space @ 400 kpc

M. Zemp
Via Lactea II

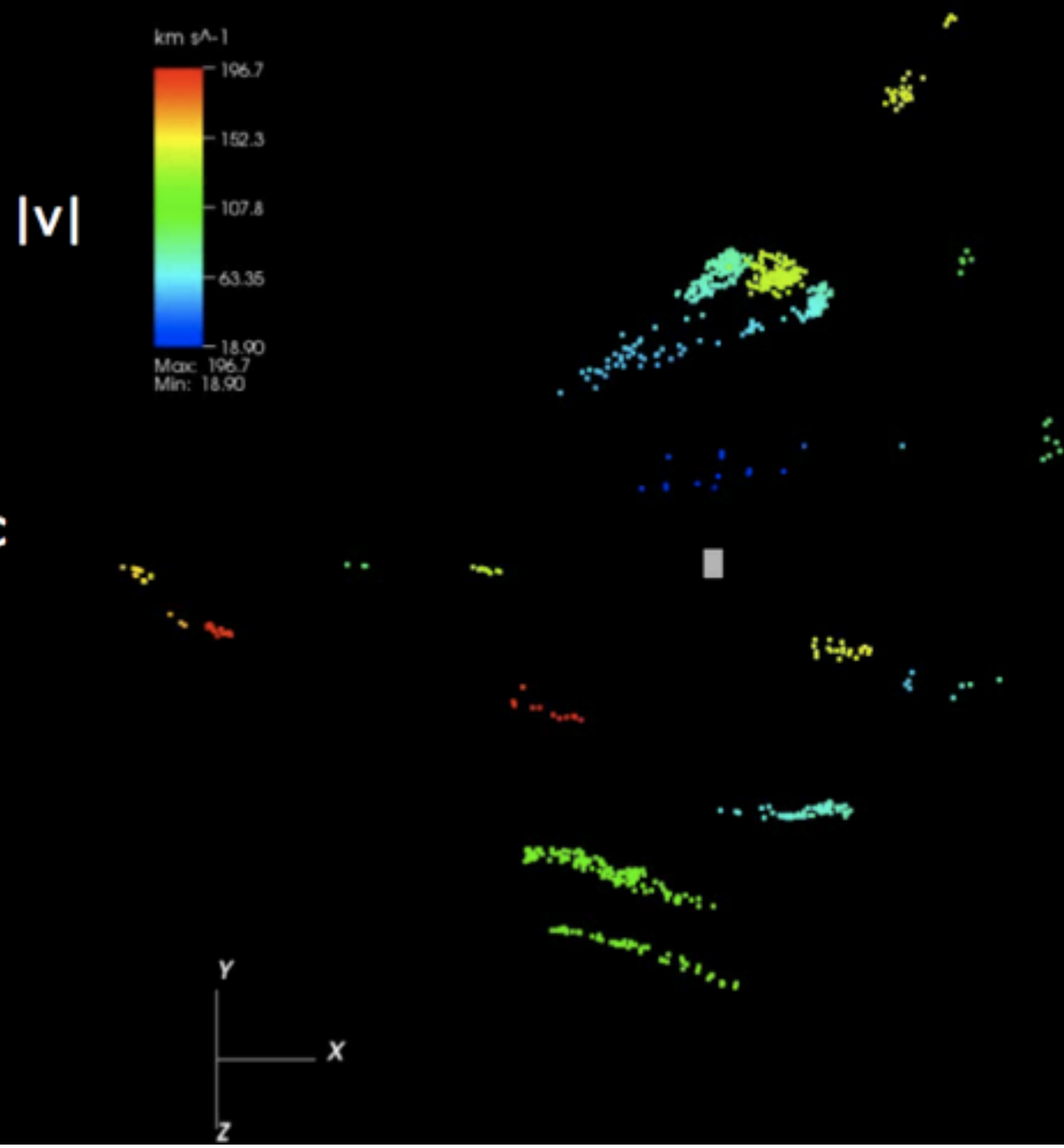

r = (0,400,0) kpc
d = 21.4 kpc

many statistics to study with cosmological N-body simulations

Bertschinger 1998

Table 1 Statistical measures applied to galaxies and numerical simulations of structure formation

Category	Statistic	Name	Reference
Particle positions	$\xi(r)$	Two-point correlation function	Peebles 1980
	$P(k)$	Power spectrum	Bertschinger 1992
	$\zeta(r_1, r_2, r_3)$	Three-point correlation function	Groth & Peebles 1977
	$B(k_1, k_2, k_3)$	Bispectrum	Peebles 1980
	$\xi_N, \bar{\xi}_N$	N-point correlation functions and moments	Peebles 1980
	$P_0(V), P_N(V)$	Void probability function, cell counts	White 1979
	—	Percolation, minimal spanning tree statistics	Coles 1992
	—	Multifractal statistics	Martínez et al 1990
Density fields	$G(\nu)$	Genus of isodensity surfaces	Melott 1990
	—	Area of isodensity surfaces	Ryden 1988
	$v_i(\nu)$	Minkowski functionals	Mecke et al 1994
	$f(\delta)$	One-point density distribution	Kofman et al 1994
	$\langle \delta_c^N \rangle$	One-point cumulants (skewness, kurtosis, etc)	Peebles 1980
	—	Shape statistics	Davé et al 1997b
Velocity fields	$f(v)$	One-point velocity distribution (and moments)	Inagaki et al 1992
	$\mathcal{M}$	Mach number	Ostriker & Suto 1990
	$f(\theta)$	Velocity divergence distribution (and moments)	Bernardeau et al 1985
	$f(v_{12}), \sigma_{12}$	Pairwise radial velocity distribution and dispersion	Davis & Peebles 1983
Redshift space	$\xi(r_p, \pi), \xi(s)$	Redshift space correlation functions	Davis & Peebles 1983
	$P_s(k, \mu)$	Redshift space power spectrum	Cole et al 1995
Clusters or halos	$n(m)$	Mass distribution	Press & Schechter 1974
	$n(V_c)$	Circular velocity distribution	Gelb & Bertschinger 1994a
	$n(\sigma)$	Velocity dispersion distribution	Evrard 1989
	$n(T), n(L)$	Temperature and X-ray luminosity distributions	Cen & Ostriker 1994a

N-body simulations of DM halos: internal structure

similarity of internal halo structure, from galaxy to cluster scales

A rich galaxy cluster halo
Springel et al 2001

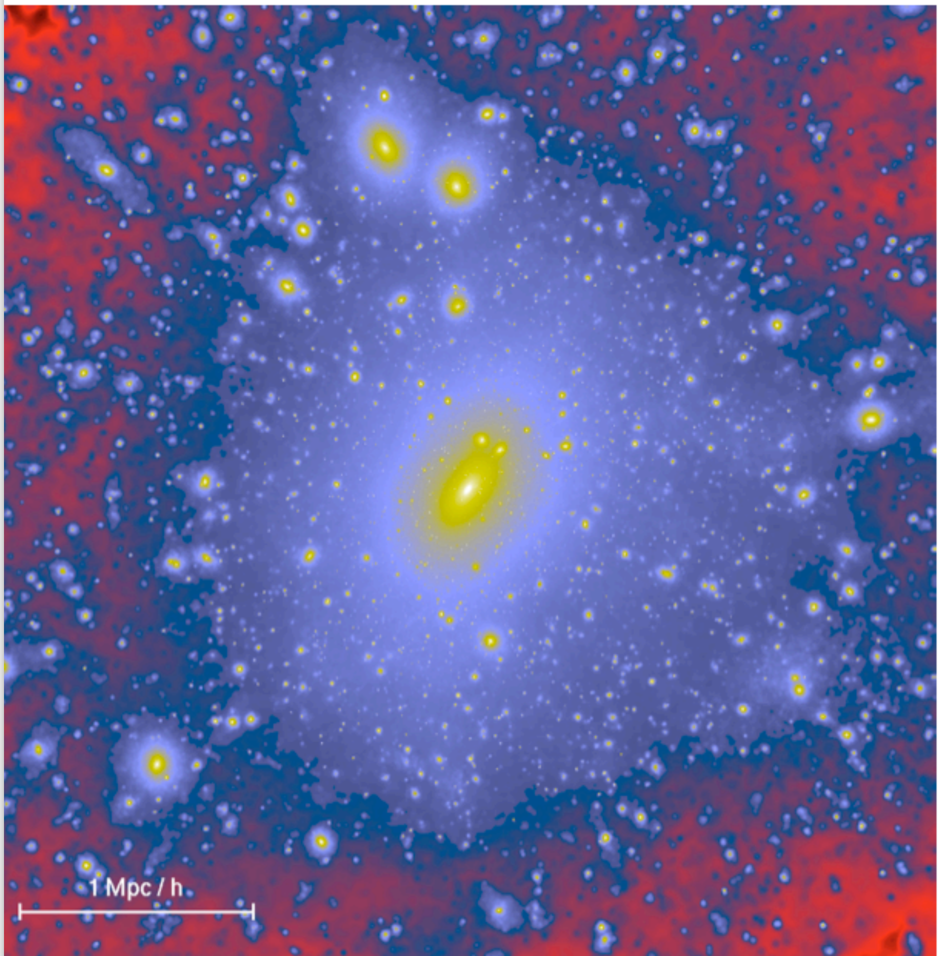

A 'Milky Way' halo
Power et al 2002

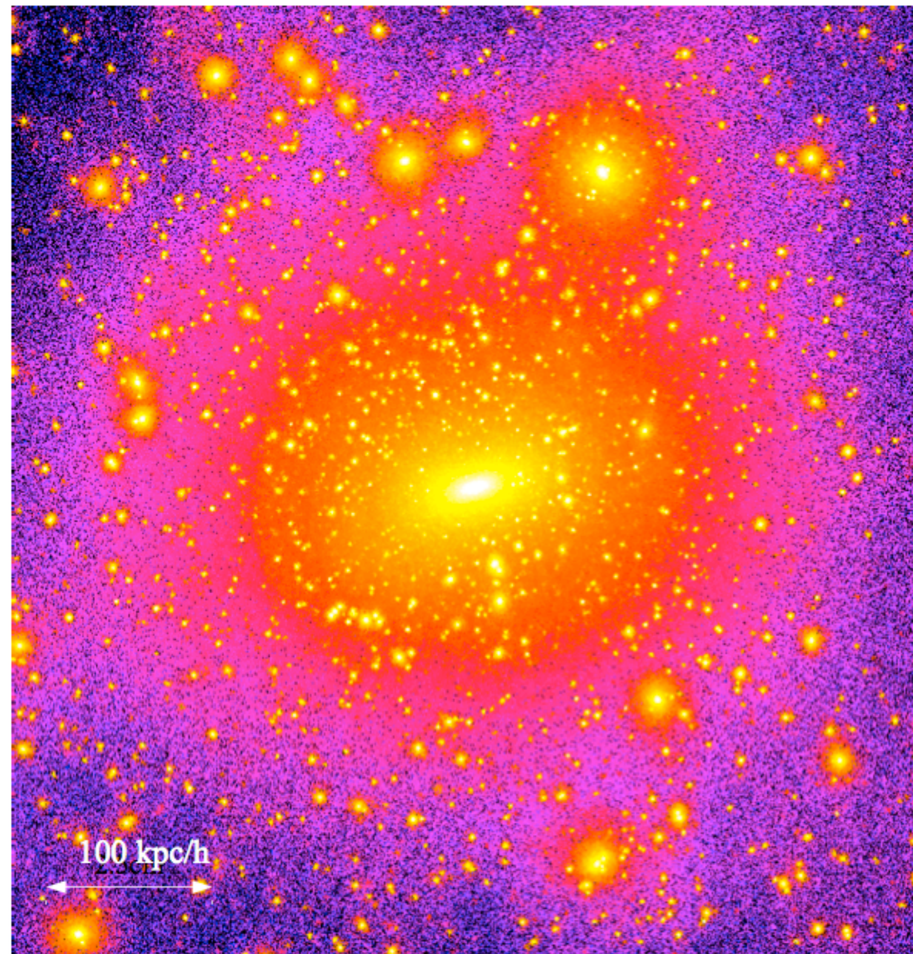

courtesy S.D.M. White, CATB2009

similarity of internal halo density profiles

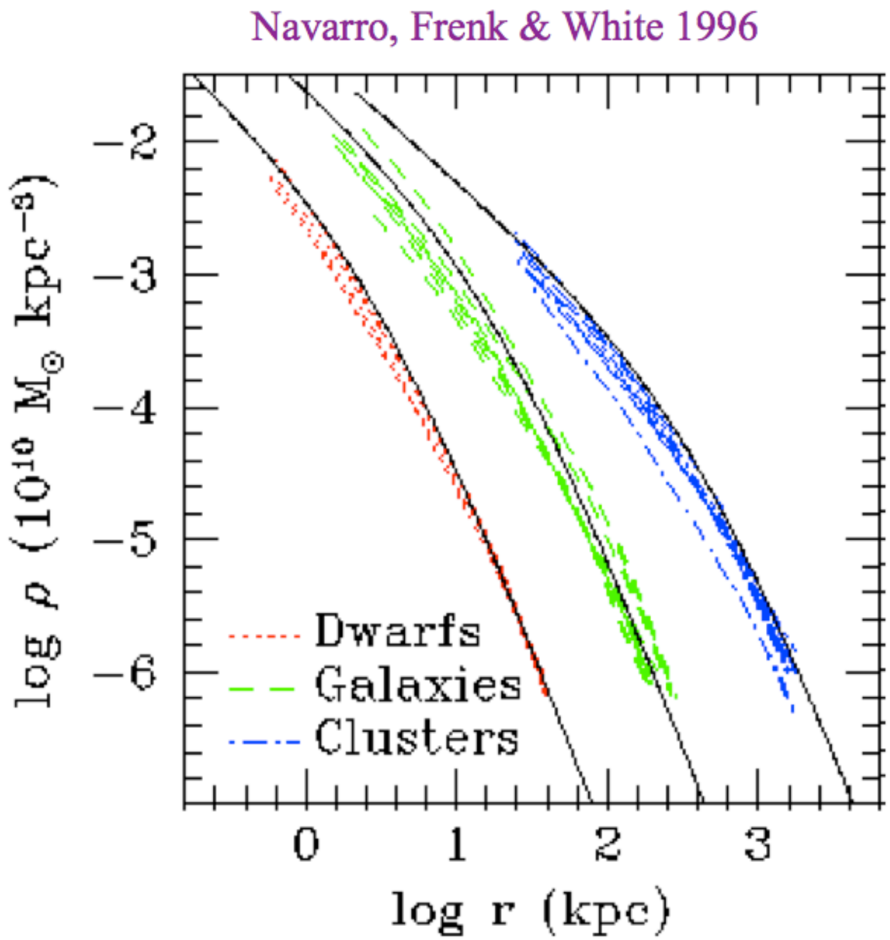

The average dark matter density of a dark halo depends on distance from halo centre in a very similar way in halos of all masses at all times

-- a universal profile shape --

$$\rho(r)/\rho_{crit} \approx \delta\, r_s / r(1 + r/r_s)^2$$

More massive halos and halos that form earlier have higher densities (bigger δ)

Concentration $c = r_{200} / r_s$ is an alternative density measure

Beware variety of definitions!

courtesy S.D.M. White, CATB2009

halo internal structure: concentration behavior

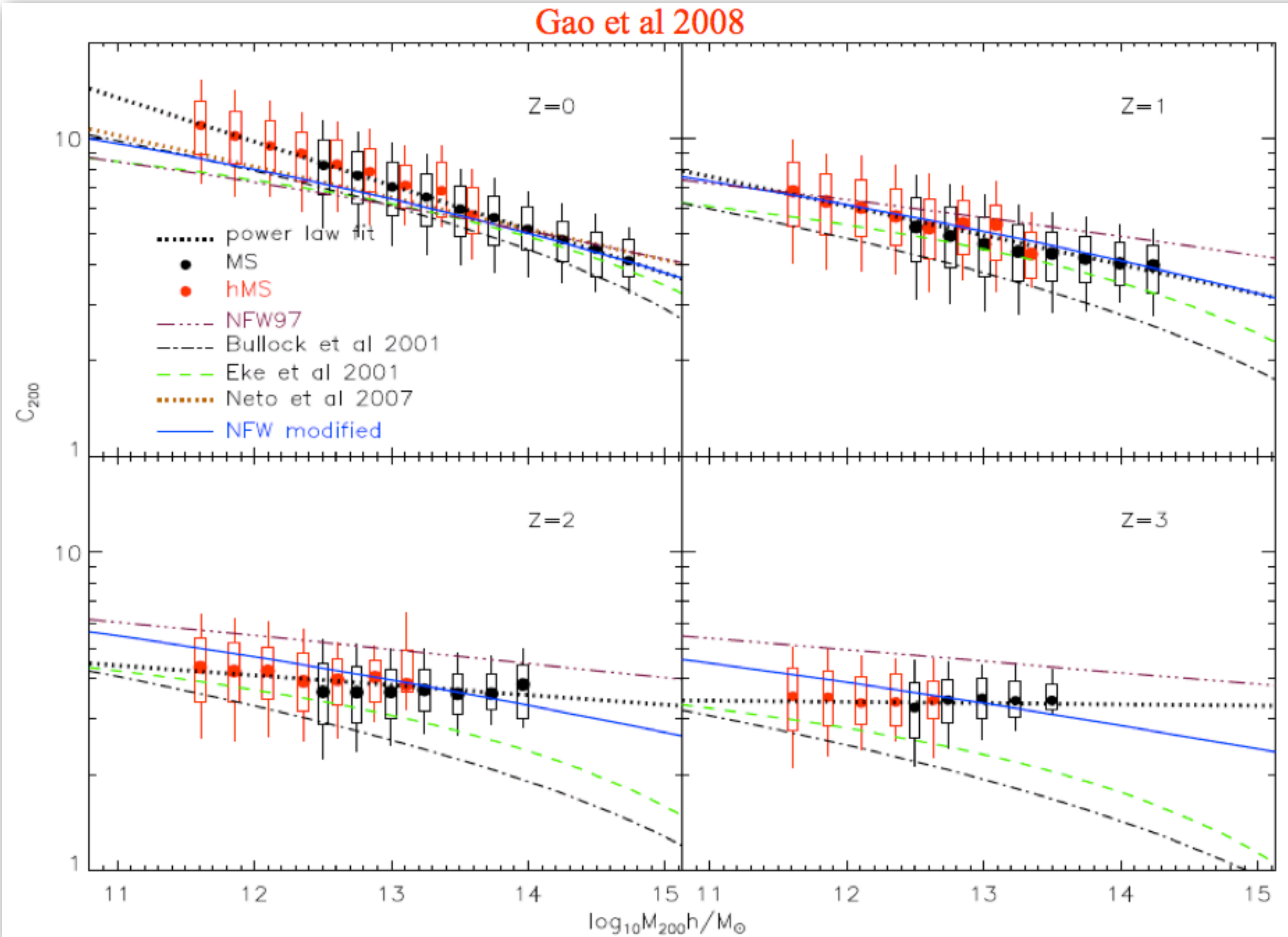

courtesy S.D.M. White, CATB2009

DM halo kinematic structure: velocity space

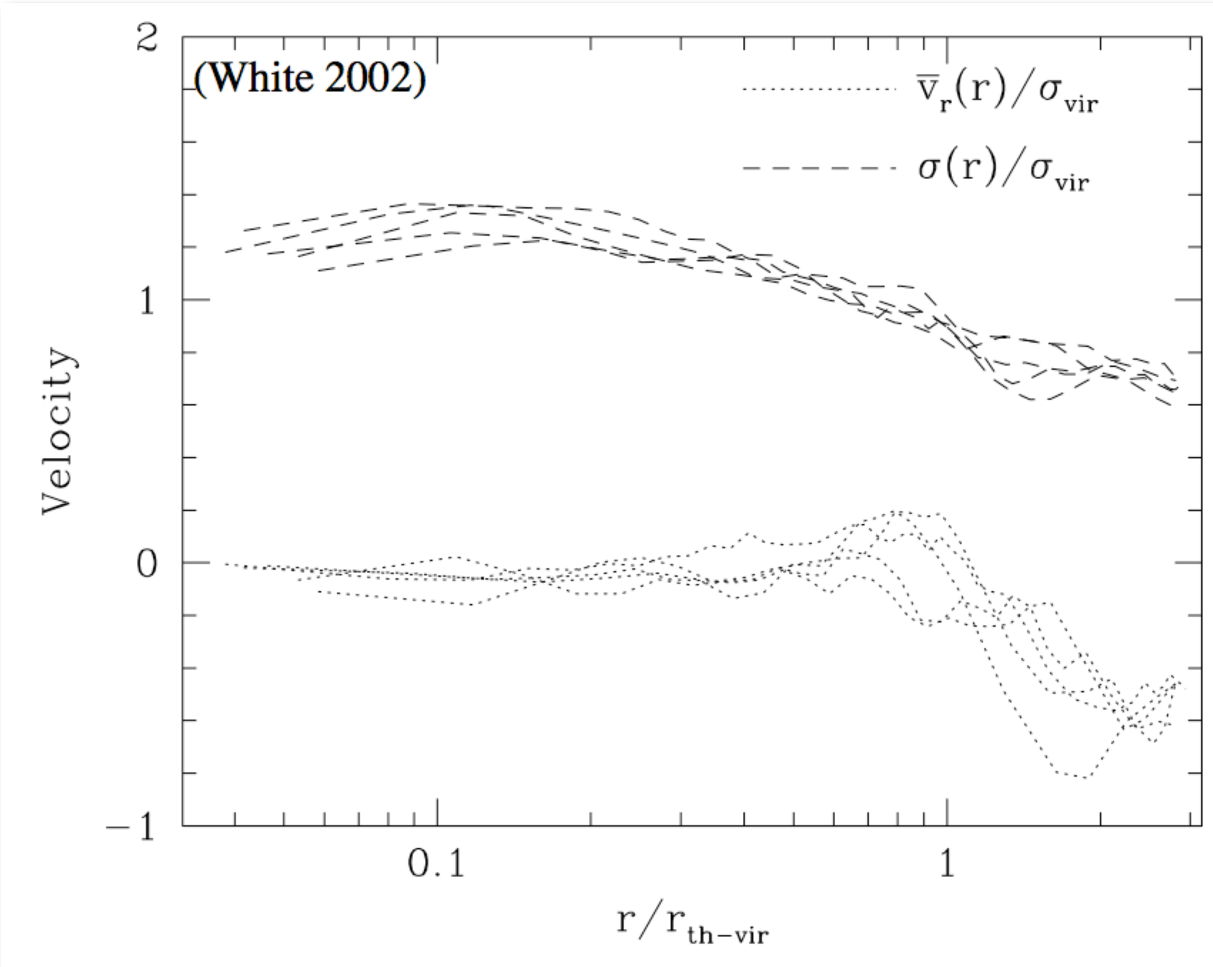

* ~hydrostatic interior $\Delta_c \gtrsim 100$

* infall outside $5 \lesssim \Delta_c \lesssim 100$

* nearly flat velocity dispersion profile

DM virial scaling relation: precision calibration

Evrard et al (2008)

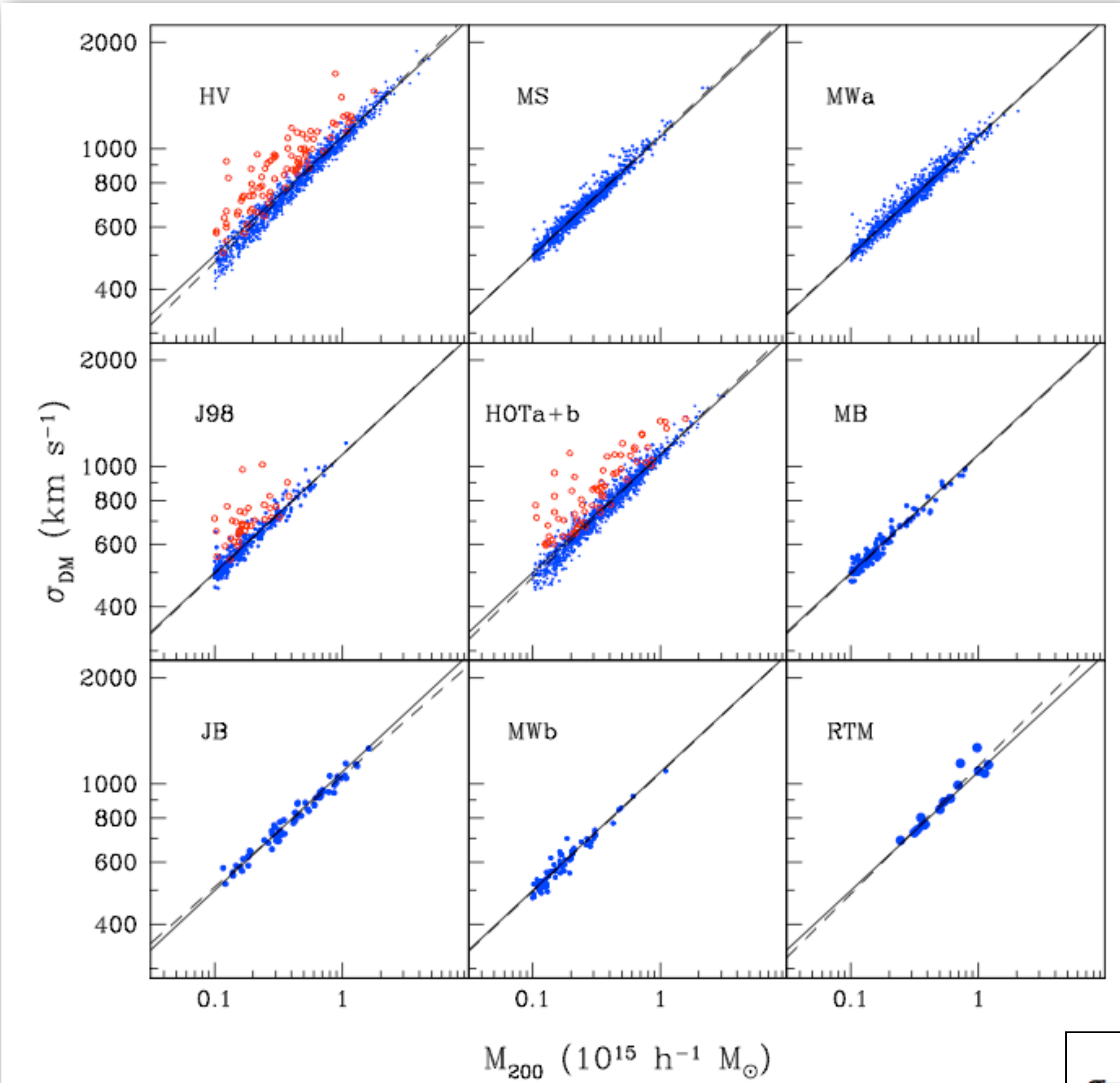

$$\sigma_{\rm DM}{}^2 = \frac{1}{3N_p}\sum_{i=1}^{N_p}\sum_{j=1}^{3}\left|v_{i,j}-\bar{v_j}\right|^2$$

* results from six different N-body codes

* mergers are relatively non-violent

$$\sigma_{\rm DM}(M,z) = \sigma_{\rm DM,15}\left(\frac{h(z)M_{200}}{10^{15}\ {\rm M}_\odot}\right)^\alpha$$

DM virial scaling relation: precision calibration

Evrard et al (2008)

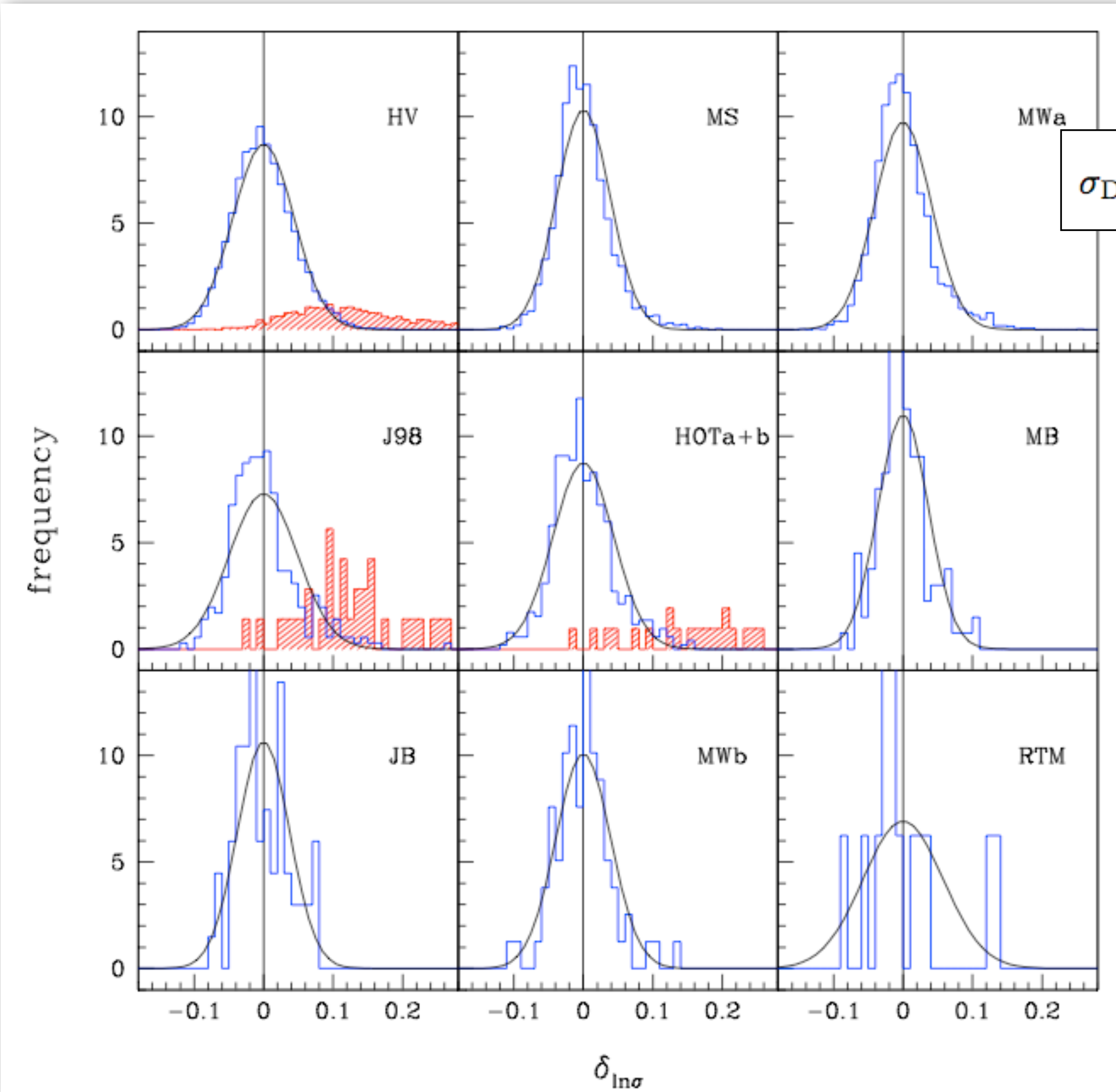

$$\sigma_{\rm DM}(M,z) \;=\; \sigma_{\rm DM,15}\left(\frac{h(z)M_{200}}{10^{15}\ {\rm M}_\odot}\right)^{\alpha}$$

* residuals from PL fit are nearly log-normal

* 4.6% scatter implies ~15% error in mass for given velocity dispersion

DM virial scaling relation: precision calibration

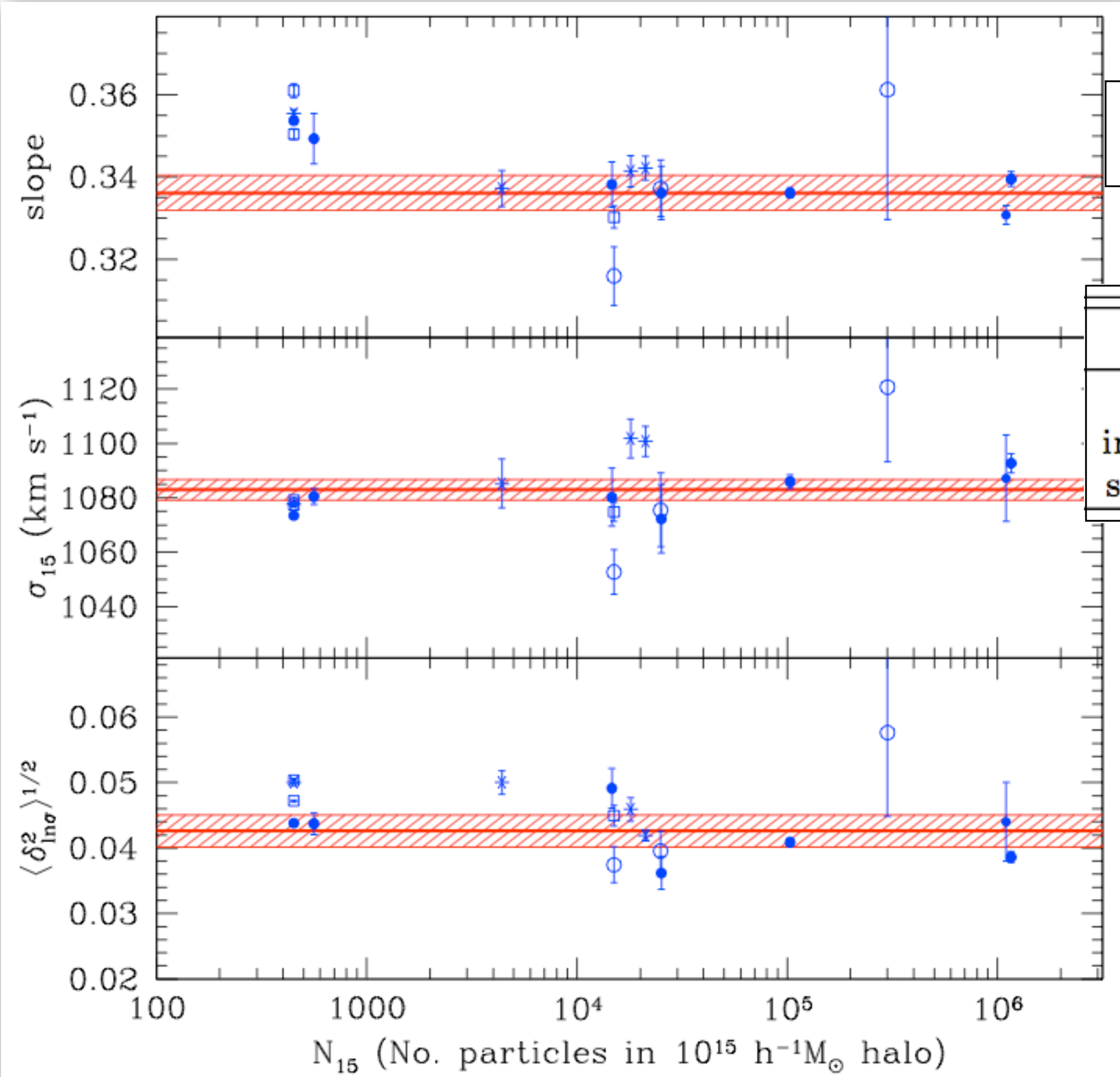

Evrard et al (2008)

$$\sigma_{\rm DM}(M,z) \;=\; \sigma_{\rm DM,15}\left(\frac{h(z)M_{200}}{10^{15}\ {\rm M}_\odot}\right)^{\alpha}$$

Parameter	Value
slope, α	0.3361 ± 0.0026
intercept, $\sigma_{\rm DM,15}$	1082.9 ± 4.0 km s^{-1}
scatter, $\langle \delta^2_{\ln\sigma} \rangle^{1/2}$	0.0426 ± 0.0015

hierarchical clustering exists within individual halos

Subhalos have subhalos have subhalos...

Springel et al 2008

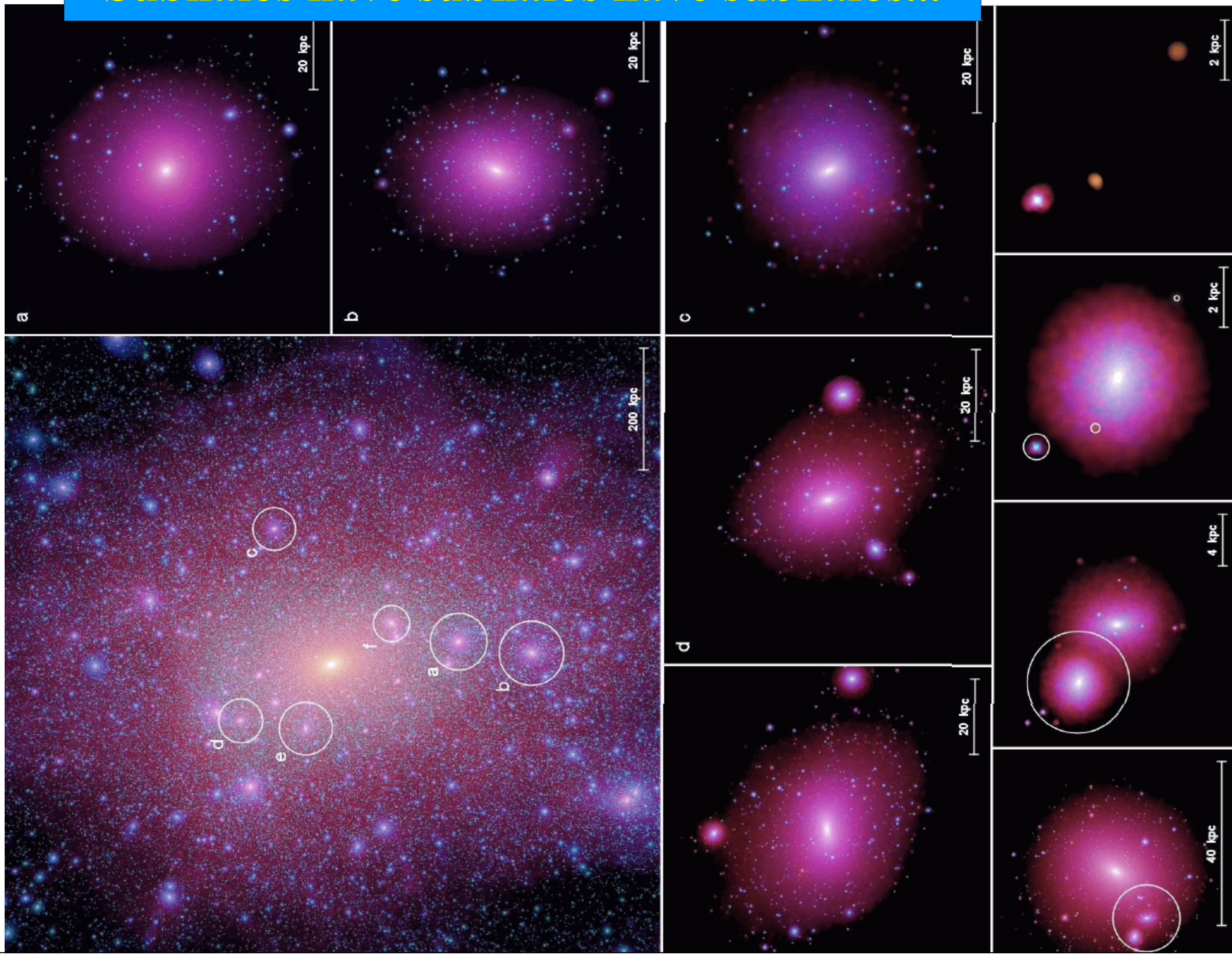

sub-halo structure ***does not dominate*** the internal density field

Density relative to a smooth ellipsoidal model

Vogelsberger et al 2008

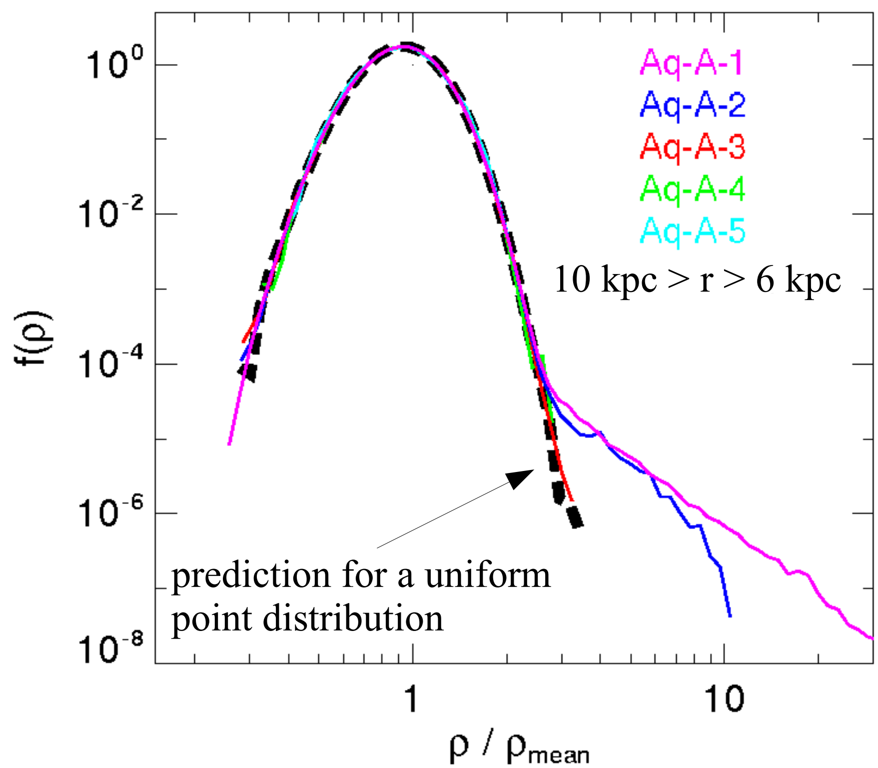

- Estimate a density ρ at each point by adaptively smoothing using the 64 nearest particles
- Fit to a smooth density profile stratified on similar ellipsoids
- The chance of a random point lying in a substructure is $< 10^{-4}$
- The *rms* scatter about the smooth model for the remaining points is only about 4%

courtesy S.D.M.White, CATB2009

halos in the sky (past light-cone) are dynamically frustrated; future is relaxed!

mean, scaled radial velocity

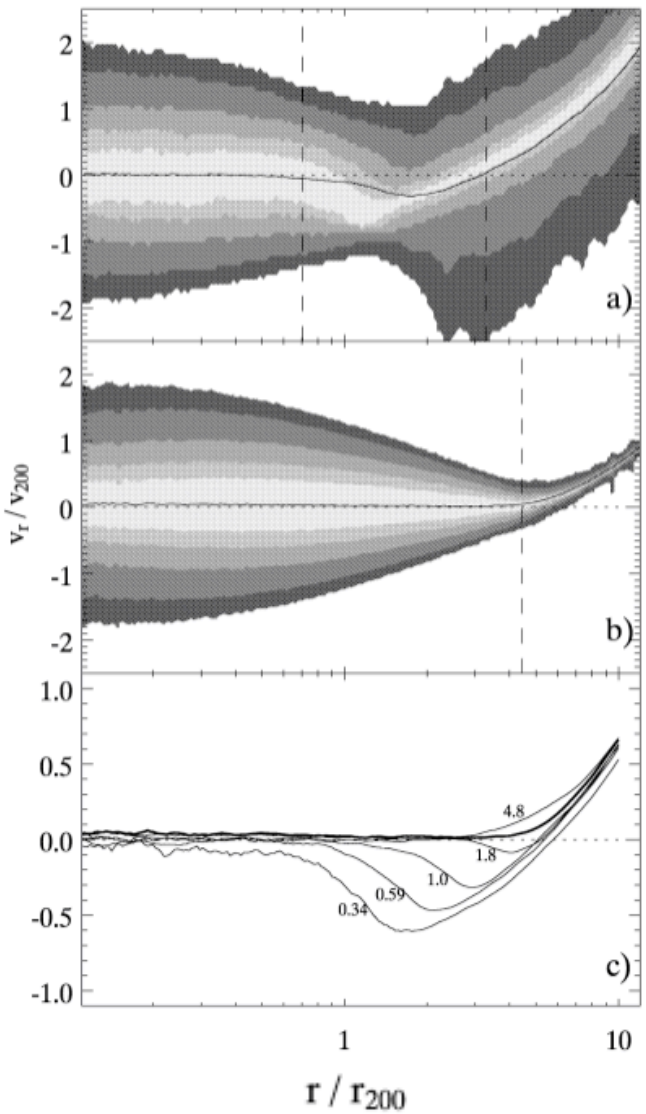

$a = 1$

$a = 100$

scaled distance from halo center

Busha et al (2005)

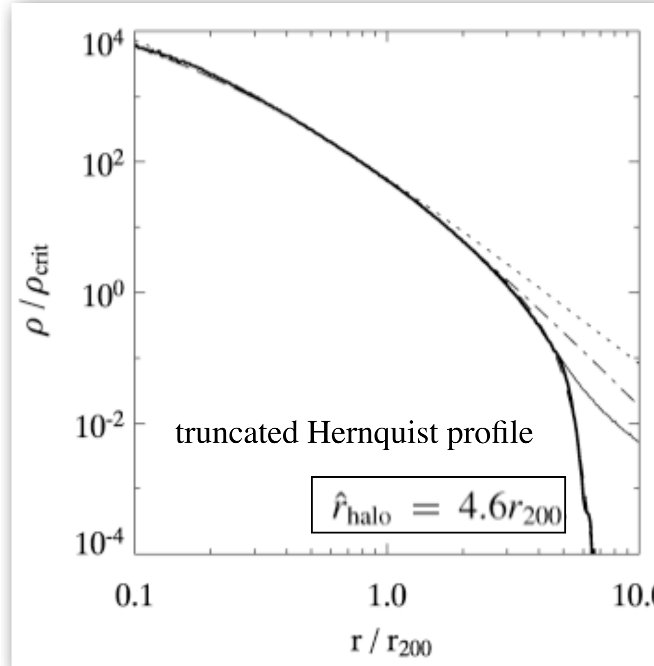

$$\rho(r) = \frac{\rho_0}{(r/r_c)(1+r/r_c)^3}\, e^{-(r/\hat{r}_{halo})^{5.6}},$$

Figure 1. The distribution of dark matter radial velocities as a function of distance from the halo centre. The top two panels show the conditional phase-space density $p(v_r \mid r)$ as a function of radius for the ensemble of 400 largest haloes at the present epoch (a) and for the future when $a = 100$ (b). The solid line shows the mean velocity as a function of radius; the grey-scale indicates the regions enclosing 40, 60, 80, 95, and 99 per cent of the particle population as specified by $p(v_r \mid r)$; the vertical lines represent the zero-velocity surfaces. Panel (c) shows the mean radial velocity for an ensemble of haloes at epochs $a = 0.34, 0.59, 1.0, 1.8$, and 4.8, with the bold line representing the function at $a = 100$.

N-body simulations of DM halos: low-order spatial statistics

web-embedded halos have fuzzy topologies => variety of mass measures

Lukic et al (2008)

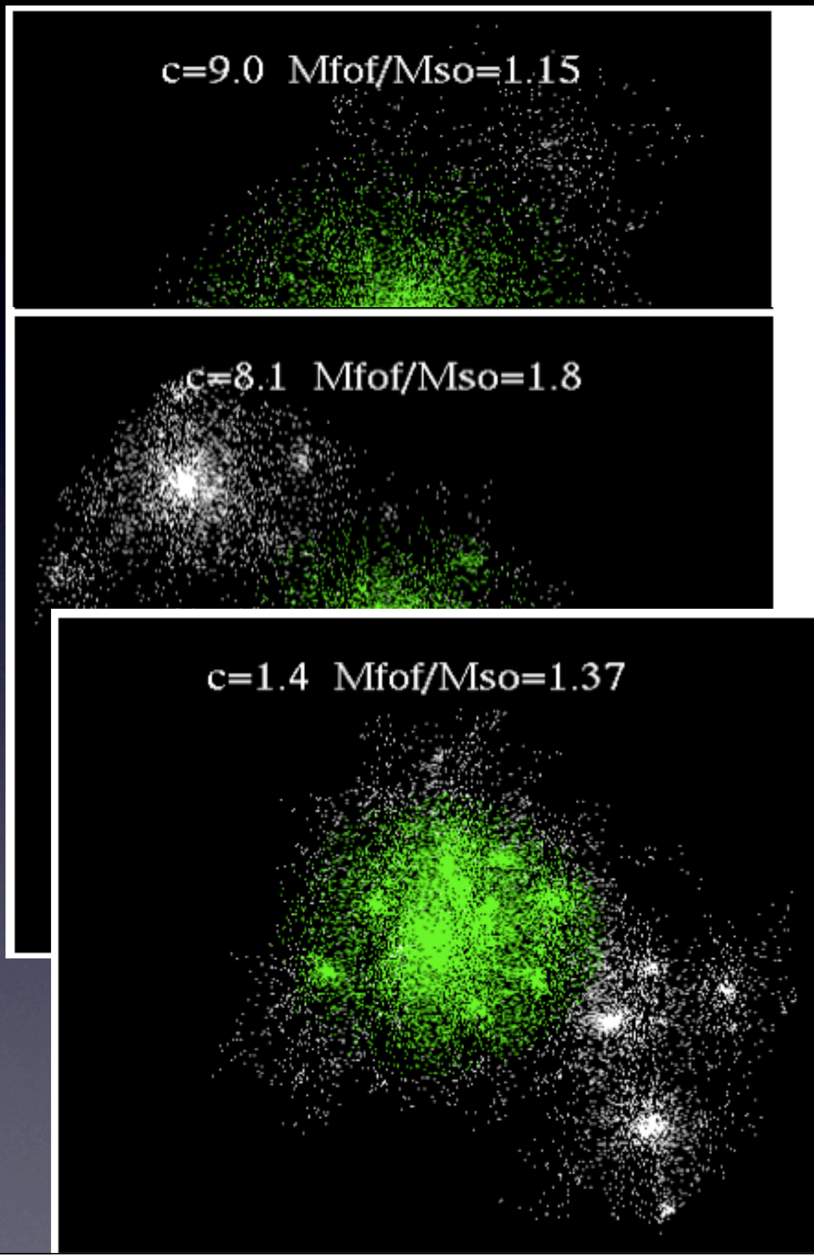

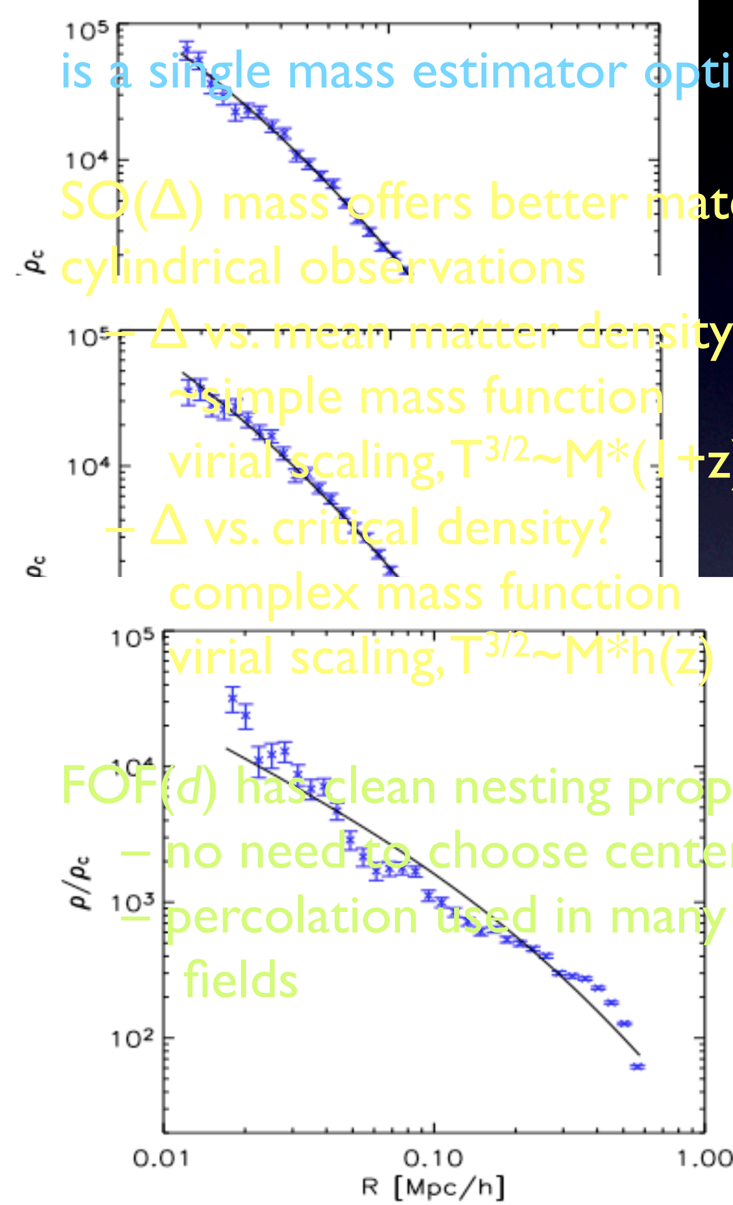

- is a single mass estimator optimal?
- SO(Δ) mass offers better match to cylindrical observations
  - Δ vs. mean matter density?
    - simple mass function
    - virial scaling, $T^{3/2} \sim M^*(1+z)$
  - Δ vs. critical density?
    - complex mass function
    - virial scaling, $T^{3/2} \sim M^*h(z)$
- FOF(*d*) has clean nesting properties
  - no need to choose center
  - percolation used in many other fields

halo space density from large N-body simulations

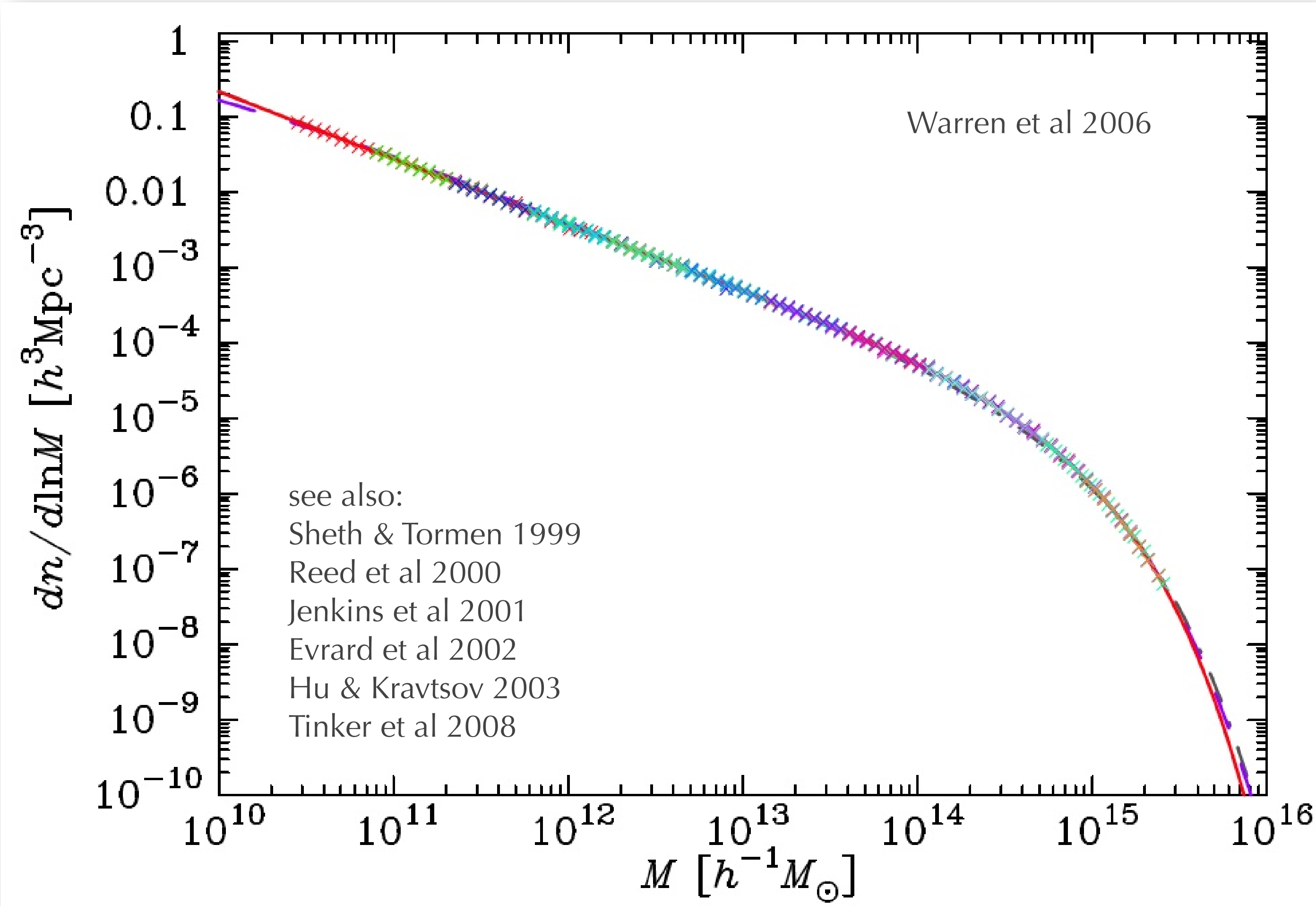

set of nine billion-particle N-body simulations

single functional form in terms of similarity variable, $\sigma(M)$, the rms density fluctuations on mass scale M

halo space density from large N-body simulations

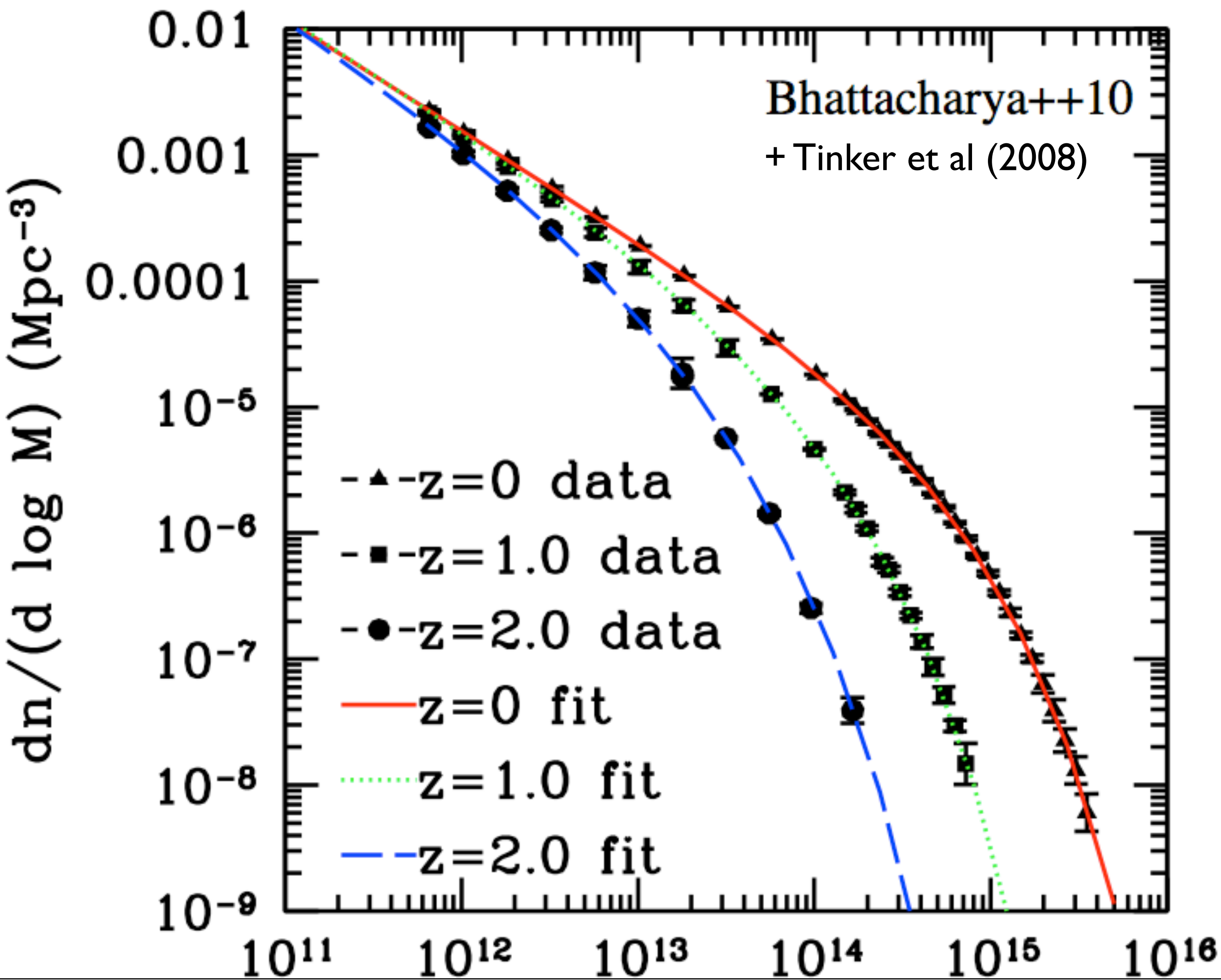

Note the dynamic range in this figure!

courtesy M. White, COTB2011

halo space density from large N-body simulations

similarity variable -
variance in filtered linear density field

$$\langle(\delta M/M)^2\rangle \equiv \sigma^2(M) = \int d^3k W_T^2(kR)P(k,z)$$

$$\frac{dn}{dM} = f(\sigma)\,\frac{\bar{\rho}}{M}\,\frac{d\ln\sigma^{-1}}{dM}$$

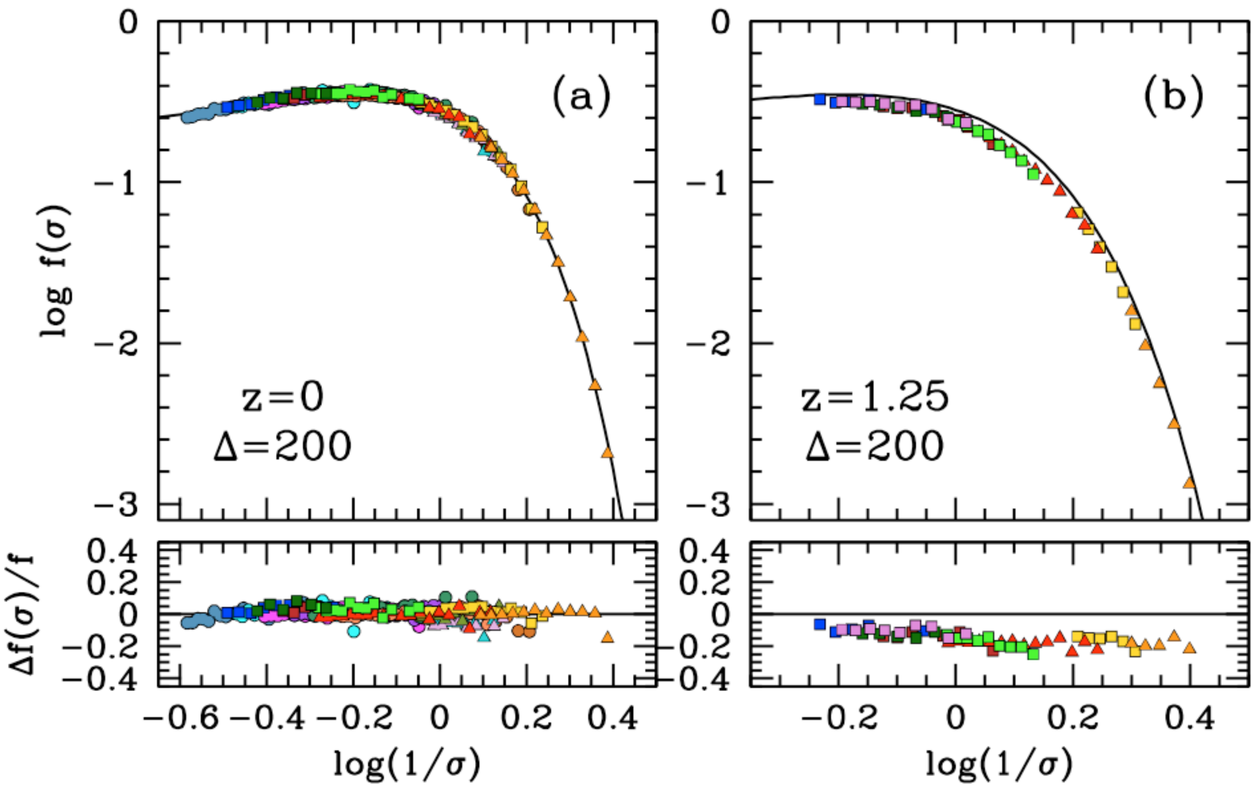

Tinker++08

22 N-body simulations with N ≥ 512^3

– 5% statistical accuracy with four parameter fit to $f(\sigma(M))$

– similarity not exact in time (need z-factors)

other fitting formulae

(A detailed study of universality and numerical issues can be found in Bhattacharya++10 from which this table is taken)

MASS FUNCTION FITTING FORMULAE DERIVED IN PREVIOUS STUDIES

Reference	Fitting function $f(\sigma)$	Mass Range	Redshift range
Sheth & Tormen (2002)	$f_{ST}(\sigma) = 0.3222\sqrt{\frac{2(0.75)}{\pi}}\exp\left[-\frac{0.75\delta_c^2}{2\sigma^2}\right]\left[1+\left(\frac{\sigma^2}{0.75\delta_c^2}\right)^{0.3}\right]\frac{\delta_c}{\sigma}$	Unspecified	Unspecified
Jenkins et al. (2001)	$0.315\exp\left[-\lvert\ln\sigma^{-1}+0.61\rvert^{3.8}\right]$	$-1.2 \leq \ln\sigma^{-1} \geq 1.05$	z= 0-5
Warren et al. (2006)	$0.7234\left(\sigma^{-1.625}+0.2538\right)\exp\left[-\frac{1.1982}{\sigma^2}\right]$	$(10^{10}-10^{15})\ h^{-1}M_\odot$	z=0
Reed et al. (2007)	$0.3222\sqrt{\frac{2(0.707)}{\pi}}\left[1+\left(\frac{\sigma^2}{0.707\delta_c^2}\right)^{0.3}+0.6G_1(\sigma)+0.4G_2(\sigma)\right] \times\frac{\delta_c}{\sigma}\exp\left[-\frac{0.764\delta_c^2}{2\sigma^2}-\frac{0.03}{(n_{eff}+3)^2(\delta_c/\sigma)^{0.6}}\right]$	$-0.5 \leq \ln\sigma^{-1} \geq 1.2$	z=0-30
Manera et al. (2010)	$f_{ST}(\sigma) = 0.3222\sqrt{\frac{2a}{\pi}}\exp\left[-\frac{a\delta_c^2}{2\sigma^2}\right]\left[1+\left(\frac{\sigma^2}{a\delta_c^2}\right)^{p}\right]\frac{\delta_c}{\sigma}$	$(3.3\times10^{13}-3.3\times10^{15})\ h^{-1}M_\odot$	z=0-0.5
Crocce et al. (2010)	$A(z)\left[\sigma^{-a(z)}+b(z)\right]\exp\left[-\frac{c(z)}{\sigma^2}\right]$	$(10^{10}-10^{15})\ h^{-1}M_\odot$	z=0-1

$$f(\sigma) = \frac{M}{\bar{\rho}}\,\frac{dn}{d\ln\sigma^{-1}} \quad , \quad \int_0^\infty d\ln\sigma\ f(\sigma) = 1$$

courtesy M. White, COTB2011

analytic underpinnings for the halo mass function

- Excursion set formalism
  - The most popular “theory”.
  - The fraction of mass in halos more massive than *M* is related to the fraction of volume in which the smoothed initial density field is above some threshold, δ_c.
  - Mass function related to random walk.
    - Press-Schechter 1974; Bond, Cole, Efstathiou & Kaiser 1991.
  - Spherical collapse vs. elliptical collapse approx.
    - Mo & White, Sheth & Tormen, Zhang & Lam, …
  - How to deal with “non-locality” of halo collapse.
- Statistics of (Gaussian) peaks plus a model for halo collapse (spherical or ellipsoidal).
    - Bardeen, Bond, Kaiser & Szalay 1986
      - Based on Rice (1944; 1945) who studied 1D Gaussian fields as models of noise in communications devices.
    - Bond & Myers 1996.
    - Dalal, Lithwick & White 201X

courtesy M.White, COTB2011

MICE (Marenostrum) calibration

Crocce et al (2009)

perco

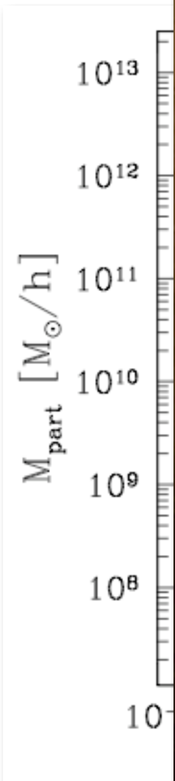

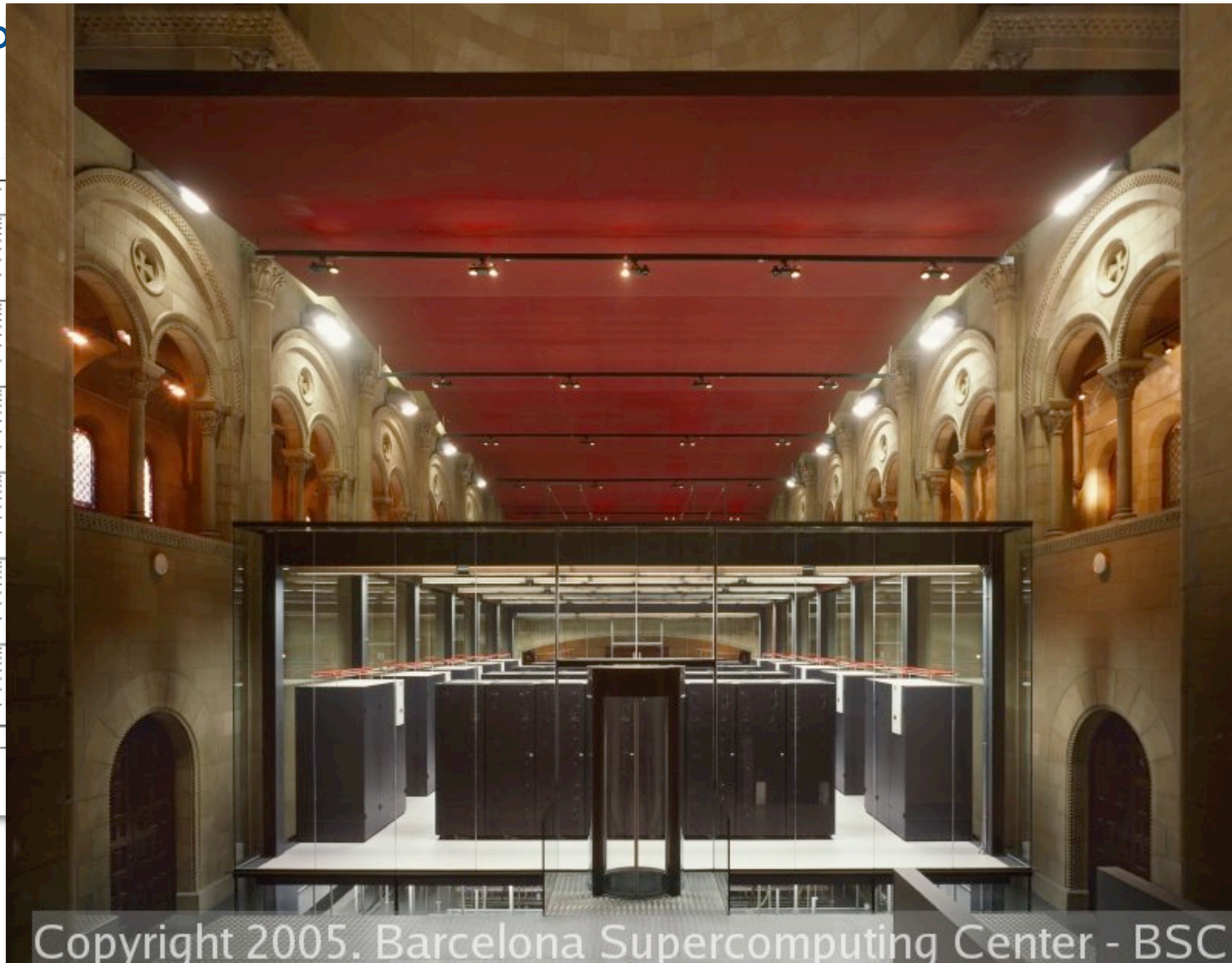

clustering of halos is ***biased*** relative to the total matter

The clustering of the rare, massive dark matter halos is enhanced relative to the general mass distribution

– Kaiser 1984; Efstathiou++88; <u>Cole & Kaiser</u> 1989; Bond++91; Mo & White 1996; Sheth & Tormen 1999; …; Tinker++10; ...

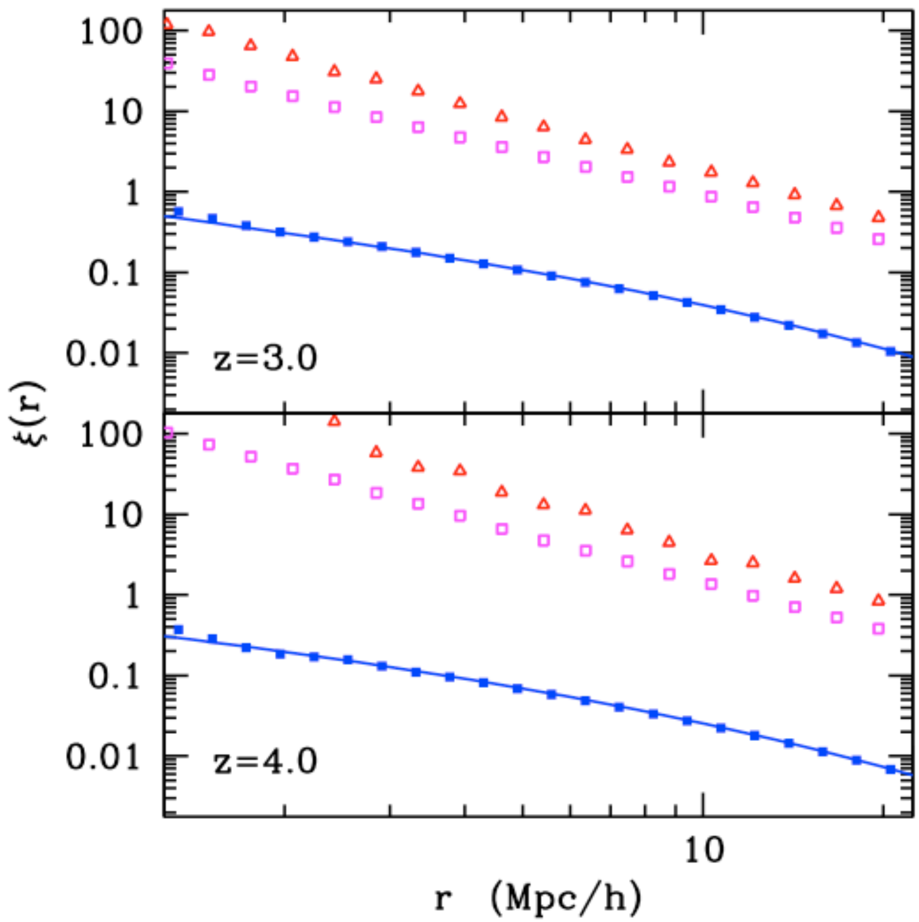

The clustering of rare halos thought to host quasars (here 10^{12} and $10^{12.5}$ M_{sun}/h) at z=3-4 is two orders of magnitude stronger than the clustering of the DM!

courtesy M. White, COTB2011

characteristics of ***biasing*** derived from simulations

This enhanced clustering is known as “bias”.

Bias depends on scale [$b(r)$], but at very large scales it becomes scale-independent [b].

- Bias, b, depends primarily on halo mass or “rarity”.
  - In simplest models $b=1+(\nu^2-1)/\delta_c$, where $\nu=\delta_c/\sigma(M)$.
  - For more accuracy, use N-body-calibrated fitting function.
  - Behavior at “extremes” can depart from fitting functions!
- Numerical simulations now large enough to test for the dependence on halo formation history and other properties.
  - Dependencies on formation redshift, internal structure, and spin.
  - Gao++05; Wechsler++06; Harker++06; Bett++07; Wetzel++07; Jing++07; Gao&White07; Angulo++08

courtesy M. White, COTB2011

bias function calibrated by large N-body ensemble (Tinker et al. 2010)

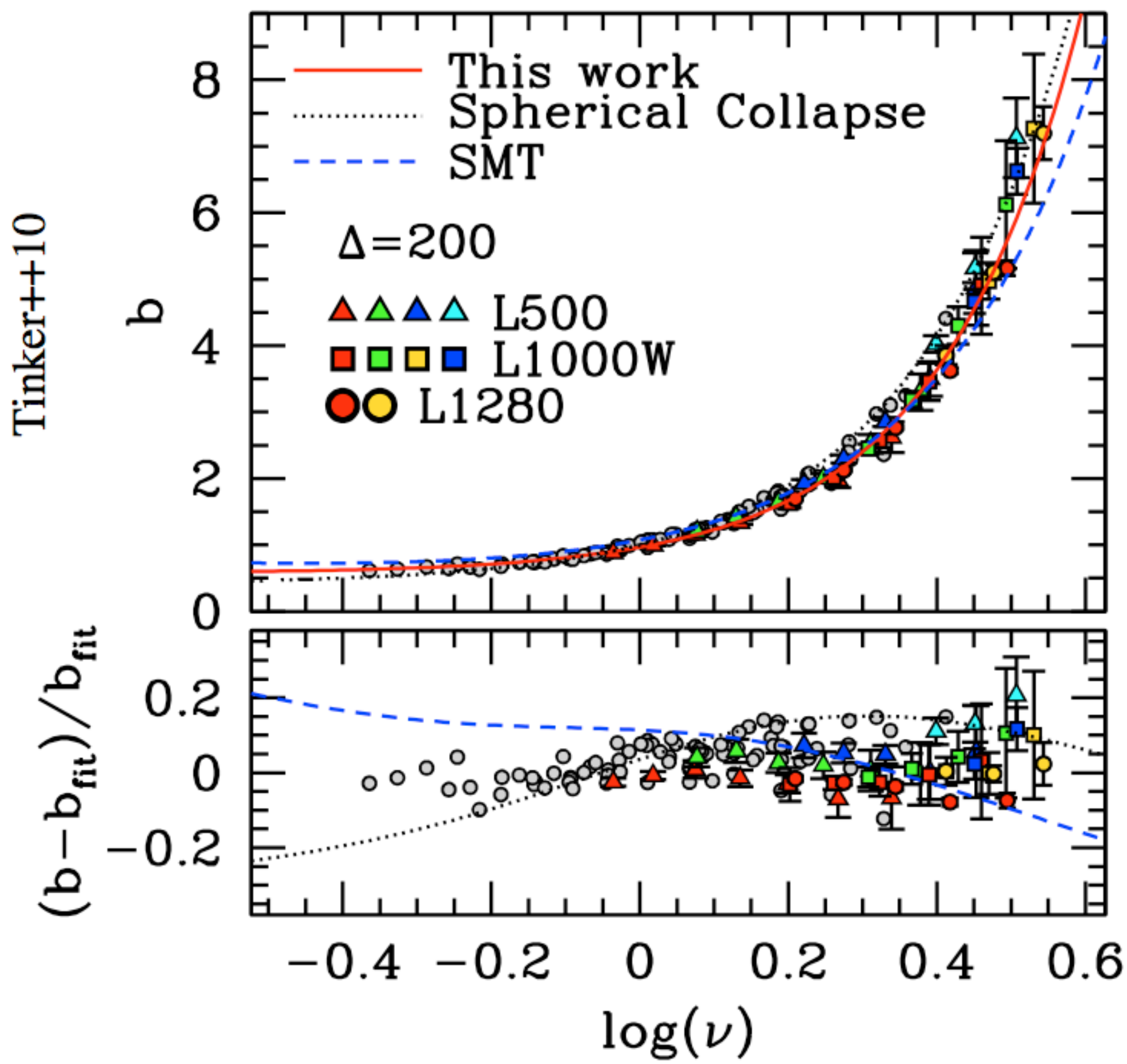

Halo bias increases with increasing halo mass at fixed redshift, or with increasing redshift at fixed mass.

courtesy M. White, COTB2011

summary: lessons from N-body simulations about ***halo model*** of LSS

* general aspects of halos

– halos are dynamically evolving systems: close to virial equilibrium but frustrated by mergers and continual accretion

– ellipsoidal in shape (tending prolate) with 2:1 axis ratios common aligned with surrounding filaments

* internal structure of halos

– relaxation to common density + velocity radial profiles

– surviving substructures contain a small percentage of total mass

– hierarchical nesting of sub-structure families reflect accretion history

* low-order spatial distribution of halos

– functional forms for *mass function*, n(M,z), and *bias function*, b(M,z), precisely calibrated via similarity variable, σ(M)   (mainly wCDM)

– different, one-parameter mass assignment methods (FOF, SO) exist
good: flexibility, reflects edge complexity   bad: literature confusing

the end